POSEIDON WATER

Appendix C
Hydrodynamic Discharge Study

Renewal of NPDES CA0109223
Carlsbad Desalination Project

Hydrodynamic Dilution Analysis for the Carlsbad Desalination Project Operating at Sixty Million Gallons Per Day Production Rate

Submitted by:
Scott A. Jenkins, Ph. D. and Joseph Wasyl
Dr. Scott A. Jenkins Consulting
14765 Kalapana Street, Poway, CA 92064

Submitted to:
Poseidon Water LLC
5780 Fleet Street, Suite 140
Carlsbad, CA 92008

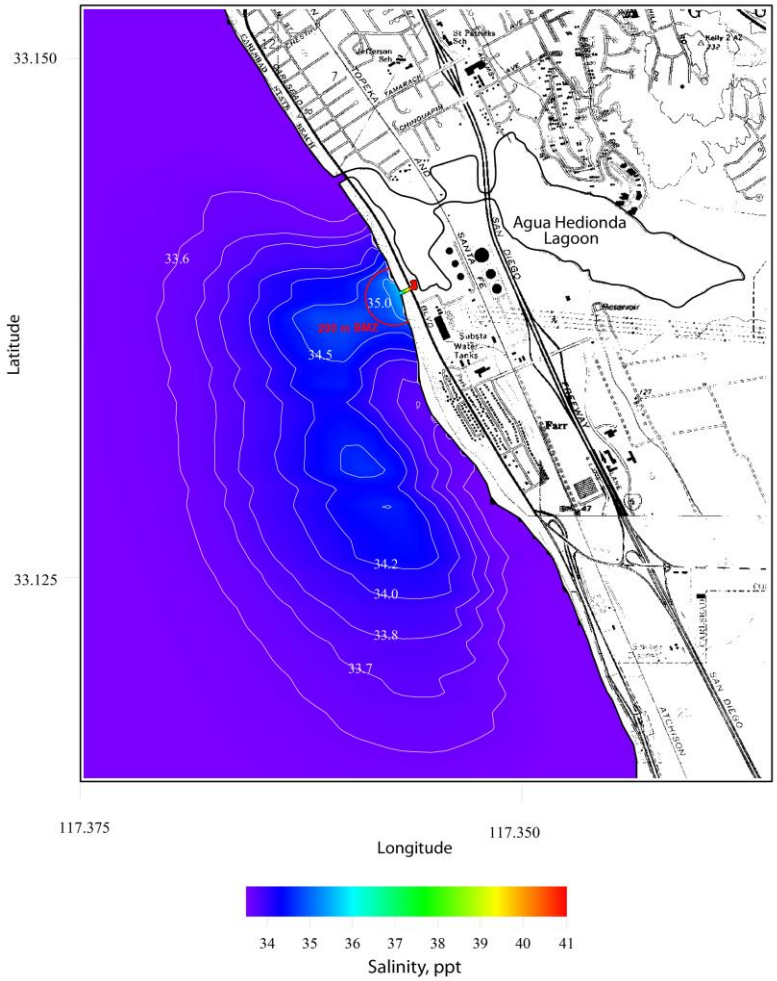

Draft: 22 July 2015; Final: 3 September 2015

EXECUTIVE SUMMARY:

We present a hydrodynamic dilution analysis related to a potential increase in product water production for the Carlsbad Desalination Project (CDP) in the light of recent amendments to the California Ocean Plan. The proposed increase in production capacity of Carlsbad Desalination Project (presently under construction at about a stage of 90% completion) would be from 50 millions gallons per day (mgd) to 60 mgd. With this increase, we examine potential compliance with a new numeric water quality objective that limits brine discharges from ocean desalination plants (whose construction are 80% complete) to no more than 2 ppt over ambient ocean salinity (*natural background salinity*) at the outer edge of a *Brine Mixing Zone* (BMZ) measuring 200 m (656 ft) in radius around the point of discharge into the receiving waters. Under this new Ocean Plan amendment, *natural background salinity* is to be determined from 20 years of ocean salinity measurements representative of the at project site.

The dilution analysis uses a process-based dilution modeling system known as *SEDXPORT* applied to a brine discharge scenario of 238 mgd of unheated brine discharged at 42 ppt salinity from the existing discharge channel at Encina Power Station, Carlsbad, CA. The EPA certified dilution models CORMIX and Visual Plumes do not contain the physics for nearshore or surf zone mixing and transport as occurs with discharges from the Encina Power Station and from the Carlsbad Desalination Project. SEDXPORT is the only available model that accounts for these coastal processes, and is the only model approved by the California State Water Resources Control Board for modeling dilution of storm drain runoff into the nearshore, (SCCWRP, 2012). Because surf zone water depths at this site constantly fluctuate due to seasonal beach profile changes and bi-annual beach disposal from Agua Hedionda Lagoon maintenance dredging, time varying bathymetry was applied to the dilution analysis based on published peer-reviewed algorithms that have been coded into the Coastal Evolution Model (CEM). Twenty year-long records of waves, currents, winds, ocean salinity and temperature were used to initialize and drive these models to produce 7,523 modeled outcomes for brine dispersion and dilution evaluated on the boundaries of a 200 m radius BMZ.

The minimum brine salinity at the 200 m BMZ boundary that was calculated from these 20.5 year-long dilution simulations is 32.8 ppt, corresponding to event days with minimum ocean salinity of 31.1 ppt. The median dilution result throughout the 20.5 year period of record gives an average brine salinity of 35.0 ppt in the plume at 200 m from the point of discharge. Altogether, 98 % of the 7,523 modeled outcomes produced discharge salinity that was less than or equal to 2 ppt above ambient ocean salinity at every point along the 200 m radius BMZ. The travel time for organisms entrained in the discharge from the outlet of the discharge pond to the point where the salinity is no greater than 2 ppt or greater over the natural background salinity is generally limited to 27 minutes. Outcomes where discharge salinity exceeded 2 ppt above daily ambient ocean salinity are extremely rare and never persistent, accounting for only 2 % of the potential discharge cases over a 20.5 year period. No modeled outcomes exceed 36.3 ppt (the upper limit of natural ocean variability) by more than measurement error, which is generally regarded as +/- 0.2 ppt using standard temperature/conductivity probes for determination of practical salinity units (psu). While hydrodynamic modeling of the CDP discharge shows a small probability (up to 2 percent) that the 2 ppt above ambient standard may be exceeded under short-term (6-hour or daily) periods, compliance with the Ocean Plan receiving water standard under minimum month conditions is assured.

Introduction:

This report supplements analysis to earlier EIR Appendix document, Jenkins and Wasyl, (2005), in response to amendments to the California Ocean Plan, as detailed in SWRCB, 2014. The present analysis uses the same methodology and hydrodynamic models of the previous EIR analysis, but takes into account the impact of three new factors that have arisen since that antecedent study. The first of these new factors is consideration of future expansion of the production capacity of Carlsbad Desalination Project (presently under construction at about a stage of 90% completion) from 50 millions gallons per day (mgd) to 60 mgd.

The second new factor considered by this study is compliance with a new numeric water quality objective that limits brine discharges from ocean desalination plants (whose construction are 80% complete) to no more than 2 ppt or 3 ppt over ambient ocean salinity (*natural background salinity*) at the outer edge of a *Brine Mixing Zone* (BMZ) measuring 200 m (656 ft) in radius around the point of discharge into the receiving waters. Under this new Ocean Plan amendment, *natural background salinity* is to be determined from 20 years of measurements of total dissolved solids (TDS) at a particular project site. This TDS specification for natural background salinity can be expressed in terms of PSU (practical salinity units), based on the recommendation of an expert science advisory panel commissioned by the California State Water Resources Control Board, (*The Brine Panel*); see SCCWRP, 2012. The PSU measurement replaces TDS because there are no long-term measurements of ocean salinity (natural background) made in terms of TDS. The PSU is derived from temperature/conductivity measurements which are an automated procedure that has existed for nearly 100 yrs. While PSU measurements are in great abundance in the oceanographic archival data bases, there are almost no historic measurements of ocean TDS in the coastal zone of California; and the handful that do exist are spotty with decadal gaps.

The third new factor accounted for under the present analysis applies to specification of the water depth in the nearfield of the discharge point, where the discharge point is in the center of the discharge channel at the end of the discharge jetties, (Figure 1a). The discharge jetties form a rip-rap walled open channel across the upper portion of the beach profile (referred to as the *bar-berm profile*). At normal tide and beach sand levels, the ends of the jetties are close to the wave break point, (Figure 2), where the bar-berm profile intersects the offshore portion of beach profile referred to as the *shore-rise profile*. (A schematic of a typical summer/winter seasonal beach profiles consisting of the intersecting bar-berm and shore rise profiles is shown in Figure 3). However, the bar-berm and shore rise profiles are in a constant state of flux due to seasonal variations in wave climate and regular additions of beach fill sands from maintenance dredging of Agua Hedionda Lagoon. Under the terms of the lagoon dredge permits, two-thirds of dredged sands are placed as beach fill on Middle and South Beach, located on either side of the discharge channel (cf. Figure 1a). The beach fill involves enormous quantities of sand, (Figure 4), typically 250,000 cubic yards every two years; which in turn makes significant changes to the beach profiles around the discharge jetties. These beach profile changes cause the local depth of water near the ends of the discharge jetties to continuously change; and those water depth variations have a significant effect on brine dilution because the volume of receiving water available for dilution is already limited by a shallow surf zone. To account for theses temporal water depth impacts on dilution, the present analysis uses a movable boundary model, The Coastal Evolution Model, (CEM), in which the beach and nearshore bathymetry is variable in response to seasonal equilibrium beach profile changes and beach disposal of Agua Hedionda

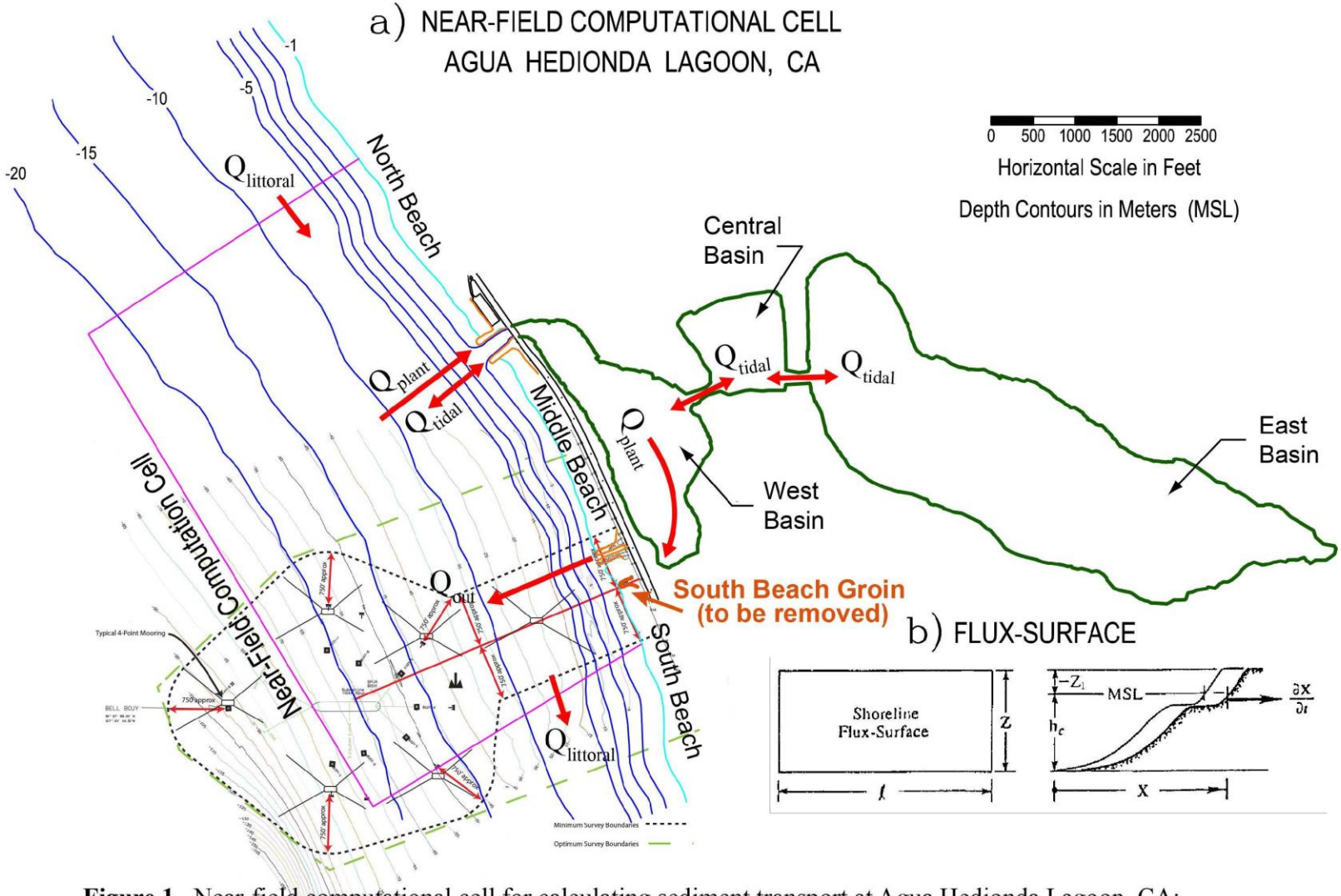

Figure 1. Near-field computational cell for calculating sediment transport at Agua Hedionda Lagoon, CA; a) Lagoon Plan View. b) Beach Cross-section.

Figure 2: Aerial view showing spatial relationship between the ends of the discharge jetties and the surf zone. (photo courtesy of NRG Energy).

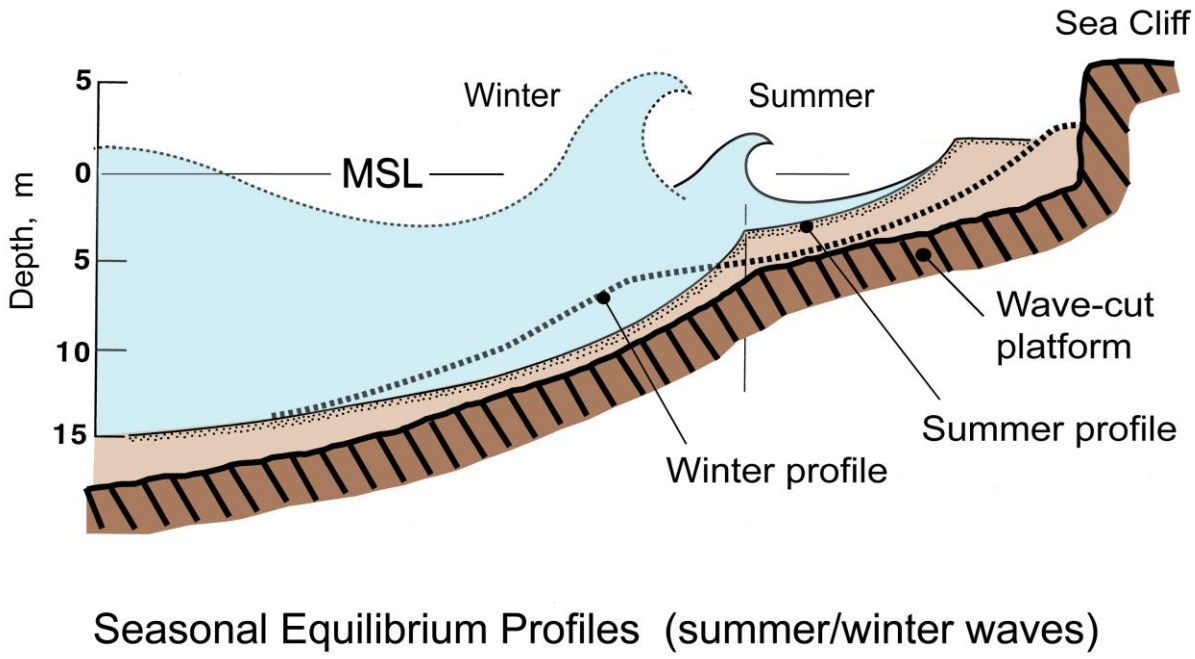

Figure 3: Schematic of summer and winter equilibrium beach profiles, from Inman, et al (1993).

Figure 4: Disposal activities of Agua Hedionda Lagoon dredge sands on South Beach. (photo courtesy of NRG Energy).

Figure 5: Google Earth image of the South Beach Groin presently located 403 ft south of the cooling water discharge channel at Encina Power Station, Carlsbad, CA.

Lagoon sands. This model is presently being used for specifying sea level rise and wave run-up design guidance to State of California, Department of Transportation, (CalTrans, 2015), and was used at this site in a 2013 NRG study of the potential beach and shoreline impacts arising from potential removal of the South Groin, (Jenkins, 2013). The South Groin is only 403 ft south of the discharge channel, (Figure 5) and the present study considers that this groin will remain in place during operations of the Carlsbad Desalination Project.

We repeat the dilution analysis of Jenkins and Wasyl (2005) found in Appendix E of the certified EIR for the Carlsbad Desalination Project. The dilution analysis uses a process-based dilution modeling system known as *SEDXPORT* applied to a brine discharge scenario of 238 mgd of unheated brine at 42 ppt salinity. EPA certified dilution models CORMIX and Visual Plumes do not contain the physics for nearshore advection and diffusion due to wave-induced shoaling, wave-induced mass transport or longshore currents and rip currents; nor due these models account for rectification of tidal boundary layers or baroclinic tidal motion. SEDXPORT

is the only available model that accounts for these coastal processes, and is the only model approved by the California State Water Resources Control Board for modeling dilution of storm drain runoff into the nearshore, (SCCWRP, 2012). The peer review record of the SEXPORT modeling system along with a technical overview are found in APPENDIX I. For the bathymetric boundary conditions, time varying bathymetry was applied to the dilution analysis based on throughput from the Coastal Evolution Model (CEM). Details of this model and how it was initialized are described in APPENDIX-II. Time varying bathymetry is an important aspect of the dilution analysis at this site, because most of the dilution occurs in the shallow surf-zone where the beach profiles and local depth of water continuously vary in response to wave climate and beach disposal of dredged sands from Agua Hedionda Lagoon (Figures 3 & 4).

2) Model Initialization:

Altogether there are six variables that enter into a solution for resolving the dispersion and dilution of the unheated concentrated seawater by-product discharged from the stand-alone Carlsbad Desalination Project. These *mixing variables* may be organized into *boundary conditions* and *forcing functions*. The boundary conditions include: the variable bathymetry from the CEM, ocean salinity, ocean temperature and ocean water levels. The forcing function variables include waves, currents, and winds.

2.1 Bathymetric Boundary Conditions: The beach and nearshore bathymetry where the Carlsbad Desalination Project discharges its brine is highly variable over time due to seasonal beach profile changes between summer and winter, and due to beach disposal of dredged sands from Agua Hedionda Lagoon. The Jenkins and Wasyl (2005) used a detailed set of post-dredging bathymetry that was measured by San Diego Gas and Electric Company (SDG&E) following the 1997-98 lagoon re-construction and maintenance dredging. All of the dredge material from this 2-year dredging program (560,000 cubic yards) was placed on Middle and South Beaches where the discharge channel is located (cf. APPENDIX-III). Typically, Agua Hedionda Lagoon is dredged every 2 to 3 years, and two-thirds of those dredged sands are placed on Middle Beach and South Beach (cf. Figures 1 -3). After each dredge disposal, the beaches are greatly built out from their equilibrium form, and large portions of dry beach extended seaward of the discharge jetties at low tide. Figure 6 shows just how significantly the bar-berm and shorerise beach profiles adjacent the discharge jetties have varied over time in response to these seasonal erosion/accretion cycles and bi-annual with dredge disposal cycles. Figure 6 shows that historically there has been as much as a 12 ft vertical change in sand levels on Middle Beach adjacent the discharge jetties between the maximum build-out following the 1998 East Basin reconstruction project when 431,259 yds^3 where placed on Middle and South Beach (APPENDIX-III), and the storm erosion of the 1993 El Nino winter. That degree of beach profile variability produces as much as 3-fold change in the available dilution water inside the 200 m radius BMZ semicircle when measured from the ends of the discharge jetties. Figure 6 also emphasizes how the use of the 1998 post dredging bathymetry in the earlier dilution study of Jenkins and Wasyl (2005), Appendix E of the certified EIR, biased the dilution results of that study toward the most pessimistic possible outcome; since the beach profiles around the discharge jetties were at an historic high-stand and dilution water volume in the BMZ semicircle

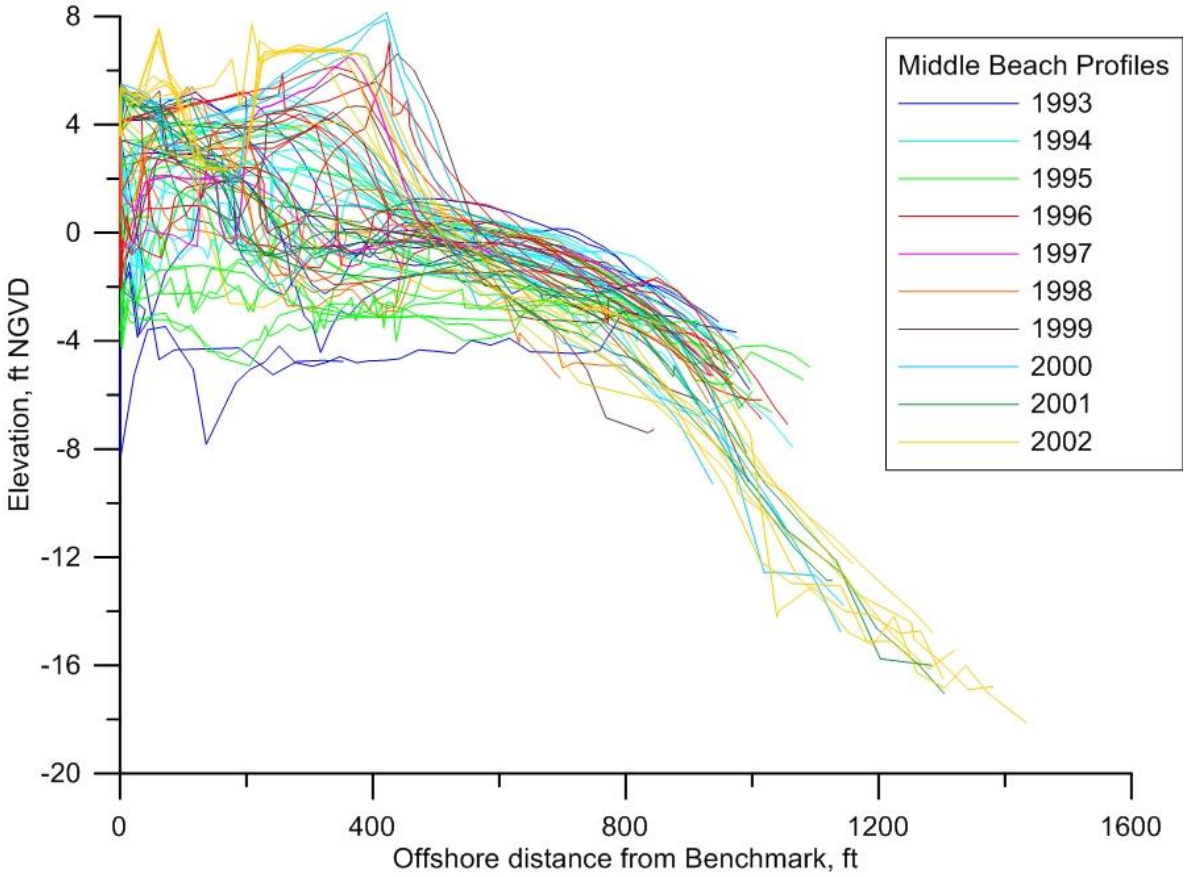

Figure 6: Cross-shore profiles of the bar-berm and shore rise profiles of Middle Beach pre- and post-dredging, 1993-2002. Data provided by William Dyson, SDG&E Dredging Department.

was at an historic minimum. For the present dilution analysis, we apply time varying corrections to the 1998 SDG&E bathymetric data set based on the elliptic cycloid representation of the equilibrium beach profile as prescribed by the Coastal Evolution Model, (see APPENDIX-II for more details).

2.2 Receiving Water Boundary Conditions and Forcing Functions: Overlapping 20.5 year-long records of the boundary condition and forcing function variables are reconstructed in Sections 3.1 and 3.2 of Jenkins and Wasyl (2005) found in Appendix E of the certified EIR (2005). These records contain 7,523 consecutive daily observations of each variable between 1980 and the middle of 2000. For clarity, these long term records are Figures 7 and 8. We search this 20.5 year period (7,523 event days) for the historical combination of the receiving ware variables in Figures 7 & 8 that give an historic average and worst case day and month, where worst-case with respect to dilution arises from benign ocean conditions that minimize mixing

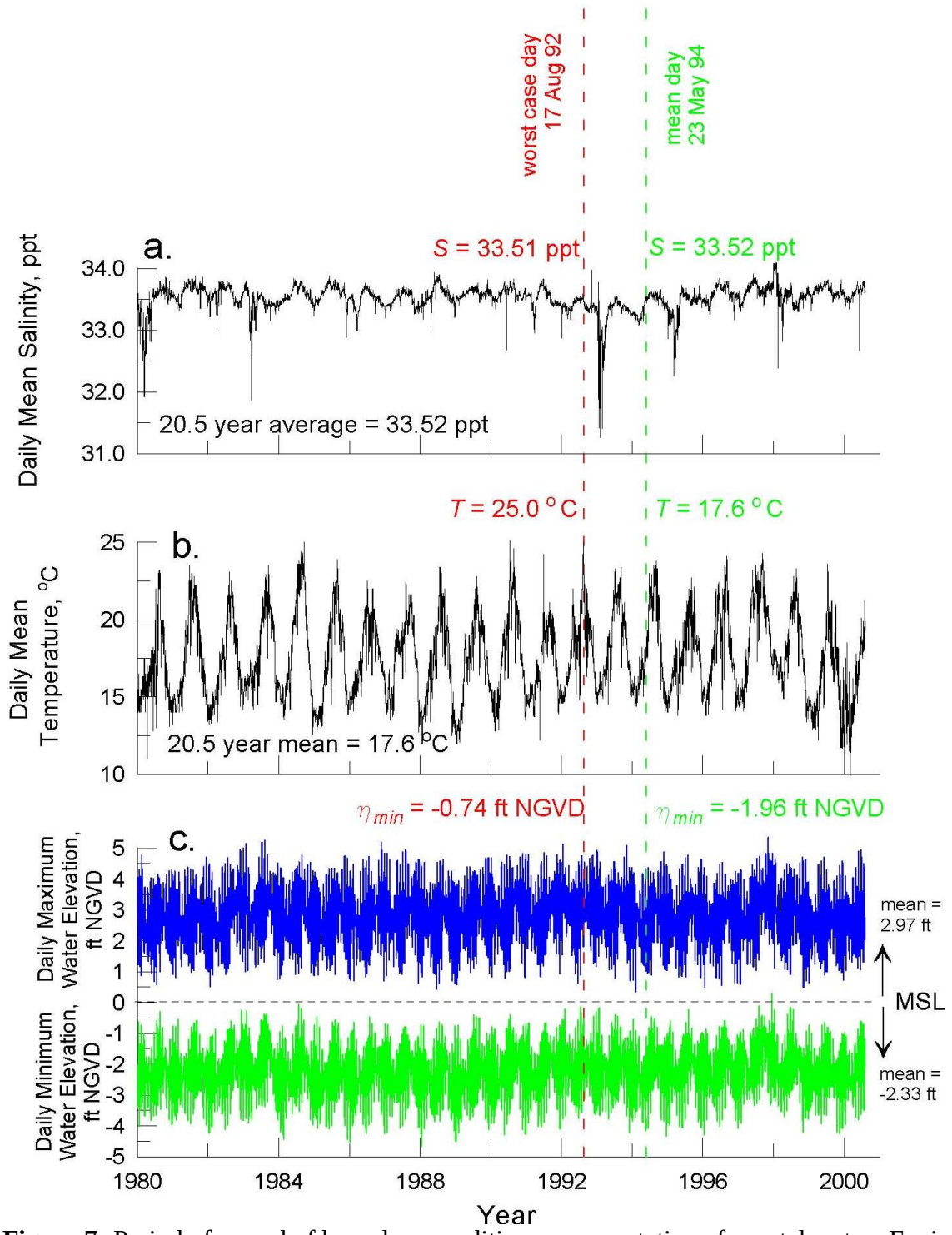

Figure 7: Period of record of boundary conditions representative of coastal waters Encina Power Station, 1980 to 2000.5: a) daily salinity, b) daily mean temperature, and c) daily high and low ocean water level. Data from Scripps Institution of Oceanography (Scripps Pier Shore Station, SIO, 2012) and the Coastal Data Information Program (CDIP, 2012).

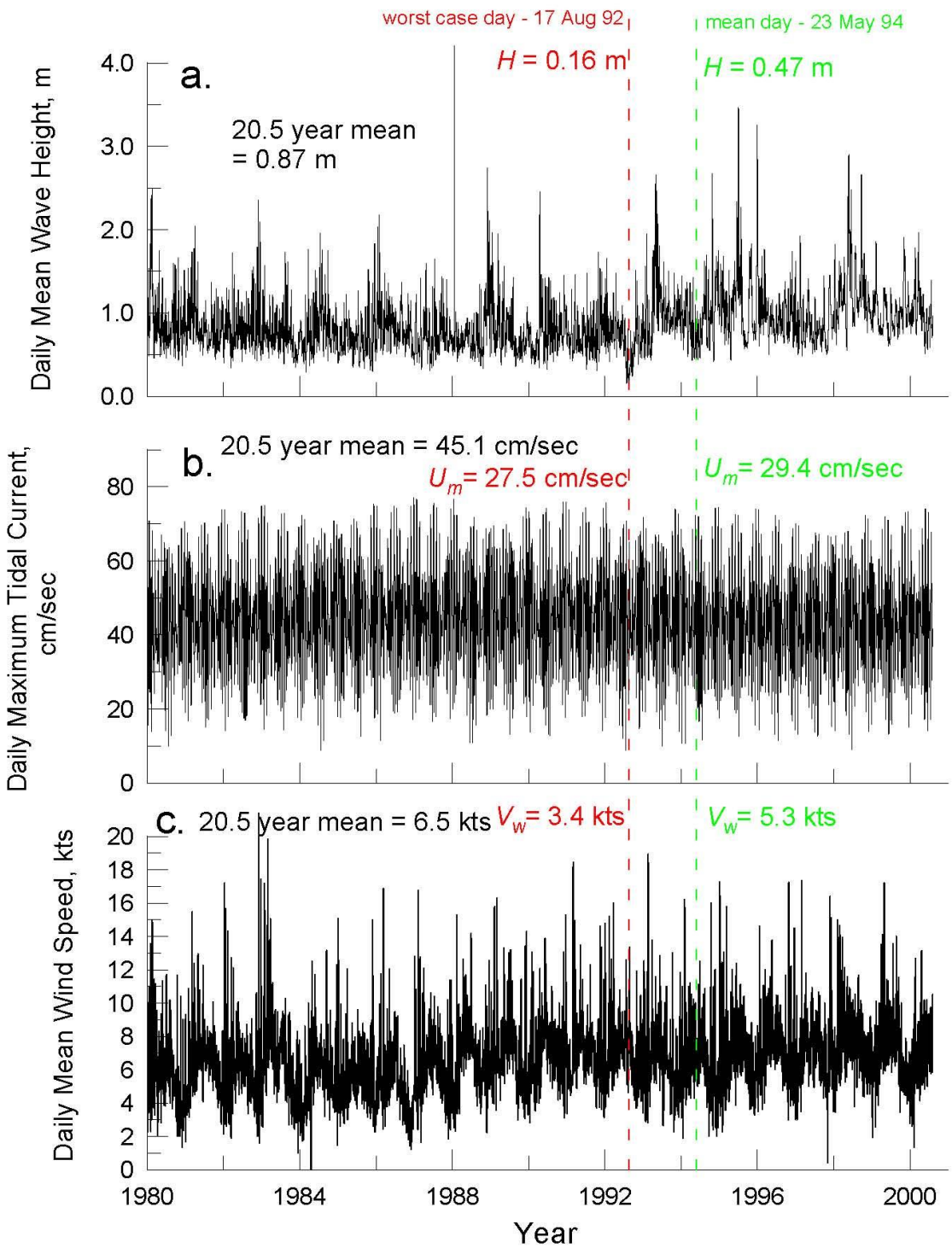

Figure 8: Period of record of forcing functions representative of the nearfield of Encina Power Station, 1980 to 2000.5: a) daily mean wave height, b) daily maximum longshore current speed, and c) daily mean wind speed. Data from Scripps Institution of Oceanography (Scripps Pier Shore Station, SIO, 2013) and the Coastal Data Information Program (CDIP, 2012).

and dilution rates. We then overlay the 238 mgd / 42 ppt brine discharge scenario on those average and worst-case (benign) ocean conditions.

The criteria for the historical worst-case day was based on the simultaneous occurrence of the environmental variables having the highest combination of absolute salinity and temperature during the periods of minimal wave, wind, currents, and ocean water levels (including both tidal oscillations and climatic sea level anomalies). The joint probability analysis produced an historical worst-case-month of August 1992, with the worst-case day represented by 17 August 1992. This day is represented by the vertical dashed red line in Figures 7 and 8. The environmental factors in August 1992 were associated with a building El Niño that subsequently climaxed in the winter of 1993. The ocean salinity on 17 August 1992 was 33.51 ppt, about the same as the long term mean, but the ocean temperature was 25.0 ^{o}C, within 0.1 ^{o}C of the 20.5 year maximum. The waves were only 0.16 m, which was the 20.5 year minimum. Winds were 3.4 knots and the maximum tidal current in the offshore domain was only 27.5 cm/sec (0.53 knots). The sluggish tidal current was due to neap tides occurring on this day with a minimum water level of -0.74 ft NGVD. This combination of environmental variables represents a situation that would place maximum thermal stress on the marine biology; and one in which the dilution of the concentrated seawater by-product of the desalination plant would occur very slowly due to minimal ocean mixing. The probability of occurrence of these worst case mixing conditions is 1day in 7,523 days, or 0.013%.

We repeat the joint probability analysis and find the closest proxy for average monthly combination of the 7 controlling variables over the 20.5 year period of record is May 1994, with representative average daily conditions occurring 23 May 1994. The average day is represented by the vertical dashed green line in Figures 7 and 8. During May 1994 the Southern Oscillation Index (SOI) was zero indicating that the climate was in a neutral phase. On 23 May 1994, ocean salinity was 33.52 ppt and ocean temperature was 17.6 ^{o}C, both identically the 20.5 year mean. Wave heights were 0.65 m, slightly below the 20.5 year mean, and maximum tidal currents reached 29.4 cm/sec (0.57 knots), also less than the 20.5 year mean. The daily low water level at -1.96 ft NGVD, very close to the mean low tide (MLT). Winds were 5.3 knots, slightly above the 20.5 year mean. Probability of occurrence of these combined 7 mean conditions is 50.01%.

Because the amended to the California Ocean Plan in SWRCB (2014) sets a water quality objective for salinity of brine discharges relative *natural background salinity*, it is important to examine the probability of occurrence statistics of natural background salinity in the coastal waters of Carlsbad, CA, as measured at the nearby Scripps Pier Shore Station (SIO 2012). Fifty years of CalCOFI monitoring of water mass properties in the Southern California Bight have shown no significant variation in salinity between San Diego and Los Angeles, CA, (CalCOFI, 2014). Hence salinity measurements at Scripps Pier in La Jolla, CA, may be considered representative of natural background salinity in the nearshore regions of Carlsbad, CA.

Figure 9 calculates the probability of occurrence (blue) and the cumulative probability of salinity from the 20.5 years (7,523 event days) of salinity measurements plotted in Figure 7. (The amended Ocean Plan requires at least 20 years of salinity data). Minimum daily salinity is 31.1 ppt and maximum daily salinity is 34.3 ppt. While the long term mean of the salinity data is 33.5 ppt, 50% of the measurements indicate salinity in the range of 33.5 ppt to 34.3 ppt. N*atural background salinity* according to the amendment is a reference location that is representative of

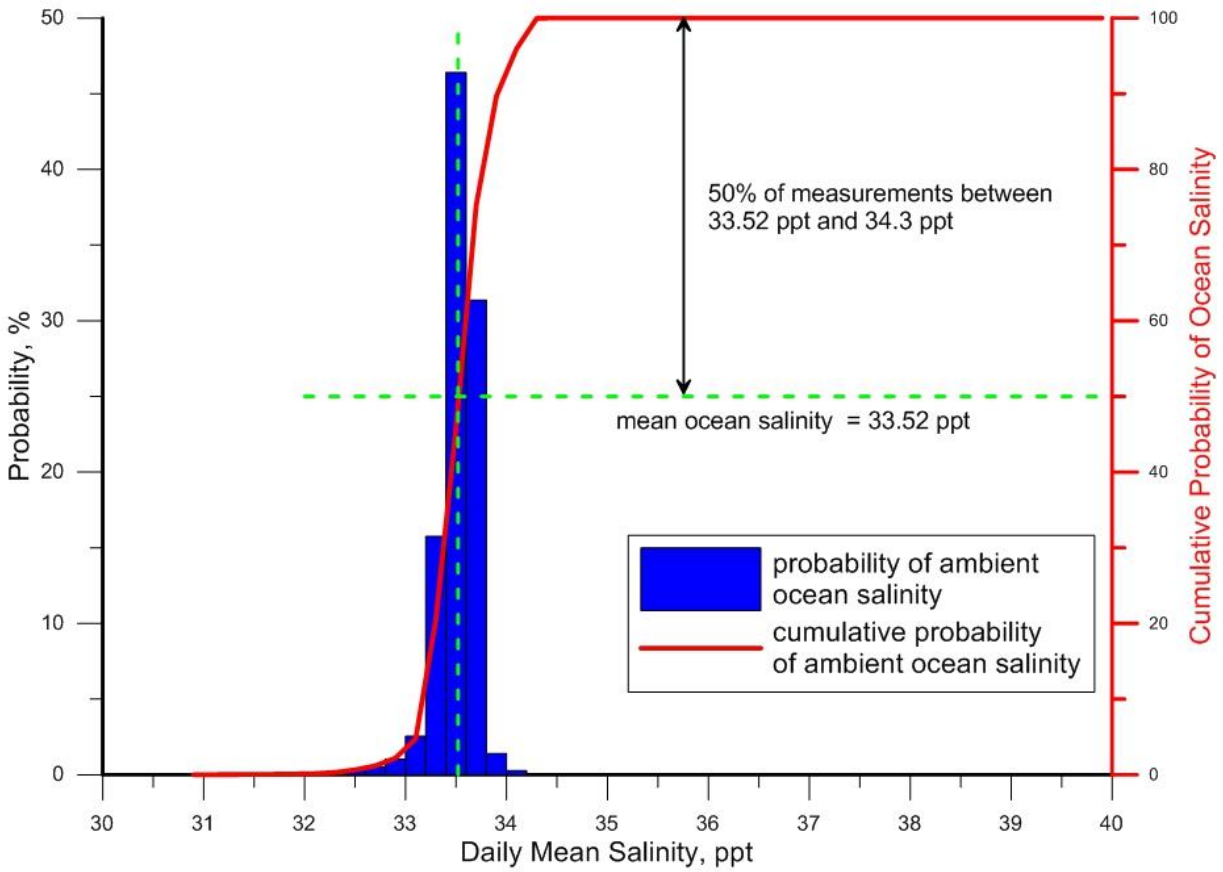

Figure 9. Probability density (blue) and cumulative probability (red) of daily mean ocean salinity in the coastal waters off Carlsbad, CA. Data from Scripps SIO Shore Station, Scripps Pier, (SIO, 2013). These records contain 7,523 consecutive daily observations between 1980 and the middle of 2000.

the *natural background salinity* of the discharge location. For the purposes of this evaluation, we have adopted the 20.5 year record at the Scripps Pier (SIO 2013) as the natural background salinity. This means that on any given day, the discharge from the Carlsbad Desalination Project must be 2ppt over the actual salinity in the historical record at 200 m from the discharge jetties.

3) Dilution Model Calibration:

The coupled sets of models were calibrated for end-to-end simulations of known dispersion events off Encina based on temperature depth profile measurements conducted over a nearshore sampling grid during February and March 1989 by Jenkins et al. (1989). This thermal plume data is shown as contour plots in Figure 10 and Appendix A of the certified EIR study of Jenkins and Wasyl, (2001). These thermal plume data were collected as part of an NPDES compliance monitoring program for Encina Power Station. It was verified by these temperature measurements that the thermal plume deflects downcoast to the south in the direction of net transport for both low and average ocean mixing conditions. Initializations for the model were derived from the historic boundary conditions and forcing functions for February and March, 1989 (Figures 7 and 8). Free parameters in the subroutines were adjusted iteratively until a best fit was achieved between the measured and simulated temperature fields.

The subroutines of SEDXPORT, (see APPENDIX I), contain seven free parameters which are selected by a calibration data set specific to the coastal type for which the hindcast simulation is run. These parameters are as follows according to the various subroutines embedded in the SEXPORT computer code:

BOTXPORT·f

*ak2 - stretching factor for vertical eddy diffusivity, ε

*ak - adjusts mixing lengths for outfalls

NULLPOINT·f

*ak7 - adjusts the asymmetry of the bedform distribution curve, μ

SURXPORT·f

*aks - adjusts the surf zone suspended load efficiency, K_s

ak4 - stretching factor for the horizontal eddy diffusivity, ε_x

RIVXPORT·f

*ak3_1 - adjusts the jetty mixing length and outfall mixing lengths

*ak3 - stretching factor for the horizontal eddy diffusivity of the discharge plume,

The set of calibration values for these parameters was used without variation or modification for all model scenarios.

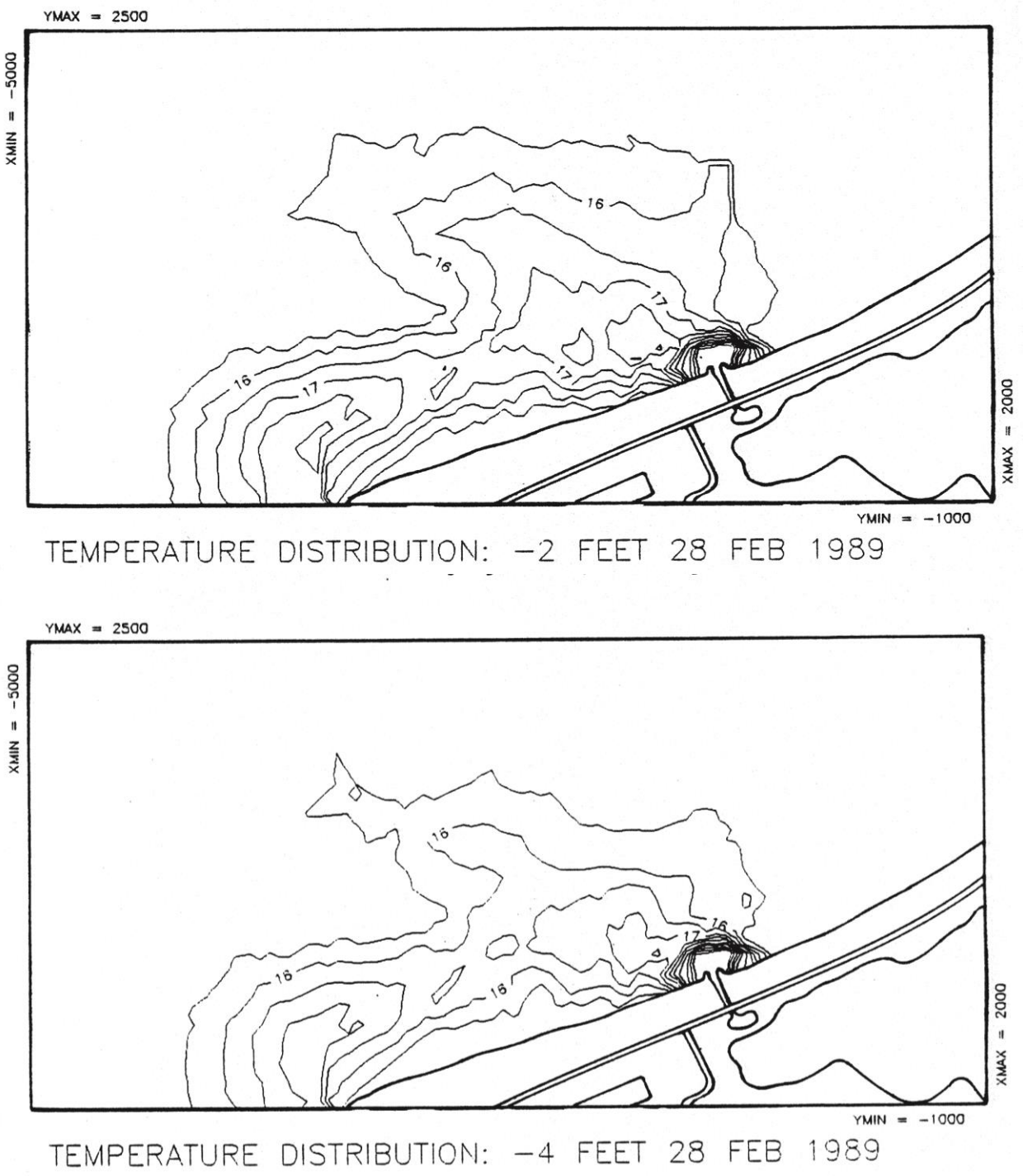

Figure 10: Encina Power Station thermal plume temperature measurements conducted over a nearshore sampling grid during February and March 1989 by Jenkins et al. (1989).

4) Dilution Modeling Results:

The SEDXPORT surfzone dilution model used in Jenkins and Wasyl (2005), Appendix E of the certified EIR was time-stepped through the 20.5 year long records of boundary conditions and forcing functions plotted in Figures 7 and 8, using time varying bathymetry from the Coastal Evolution Model after Jenkins 2013. The desalination operating scenario was based on a combined intake flow rate of 298 mgd, with 238 mgd being discharged into the ocean discharge channel at a salinity of 42 ppt after blending with the concentrated sea salts from the desalination plant. No power generation is assumed so that the Delta-T of the pre-diluted brine relative to ocean water temperature is $\Delta T = 0^0$ C.

4.1 Results for Average Daily Event: Figure 11 gives the brine plume dispersion on the seabed under average-ocean mixing/advection conditions. Because the 42 ppt discharge is heavier than ambient seawater the highest salinity in the brine plume occurs on the seabed as contoured in Figure 11. Historically, the proxy day for average-ocean mixing/advection conditions is represented by 23 May 1994.The salinity field is time averaged over 24 hours and contoured in parts per thousand (ppt) according to the color bar scale at the figure. The brine plume is asymmetric and exhibits a southerly displacement due to the prevailing net southward longshore current as a consequence of wave shoaling and tidal rectification with ebb-flow dominance towards the southeast. (This same behavior was observed in the dispersion of the Encina thermal plume used for model calibration, cf. Figure 10). Maximum salinity on the seabed in the surf zone receiving waters reach 38.7 ppt extending 26 meters offshore of the discharge jetties and covering an area of 0.5 acres of the sub-tidal beach face and sandy bottom nearshore habitat. At 200 m from the discharge point, (on the southern edge of the BMZ) salinity is 35.0 ppt, effecting an area of about 5.3 acres out of a total area of 15.5 acres enclosed by the 200 m radius BMZ. In the water column, (Figure 12), salinity in the brine plume is significantly less due to surf zone turbulent mixing and negative buoyancy effects which act to confine the plume to a bottom boundary layer. Figure 12 indicates that maximum depth-averaged salinities reach 35.9 ppt directly seaward of the mouth of the discharge channel and decline to only 33.7 ppt along the 200 m BMZ boundary under average daily-ocean mixing and advections conditions. Thus the discharge limits of the newly amended Ocean Plan are satisfied on both the seabed and in the water column under average daily conditions.

4.2 Results for Worst-Case Daily Event: Figure 13 gives the brine plume dispersion on the seabed for the worst-case day among 7,523 modeled event days. Historically, this result is represented by the ocean conditions on 17 August 1992. Because of the warmer ocean water during these summer El Nino conditions, the brine is even more negatively buoyant than for the average event day in Figure 11; and that fact in combination with extremely small breaking waves (wave height = 0.16 m) and minimal surf zone turbulence during worst-case conditions causes the brine plume to become confined to the immediate neighborhood of the seabed in a thin bottom spreading layer that tends to flow downslope and offshore along the beach bottom gradients. There is however a southerly drift due to the tidal currents with ebb dominance towards the southeast, so that the brine plume is still somewhat asymmetric and exhibits a southerly displacement, although to a lesser degree than for the average event day in Figure 11. Maximum salinity in the surf zone receiving waters reach 40 ppt exposing about two thirds,

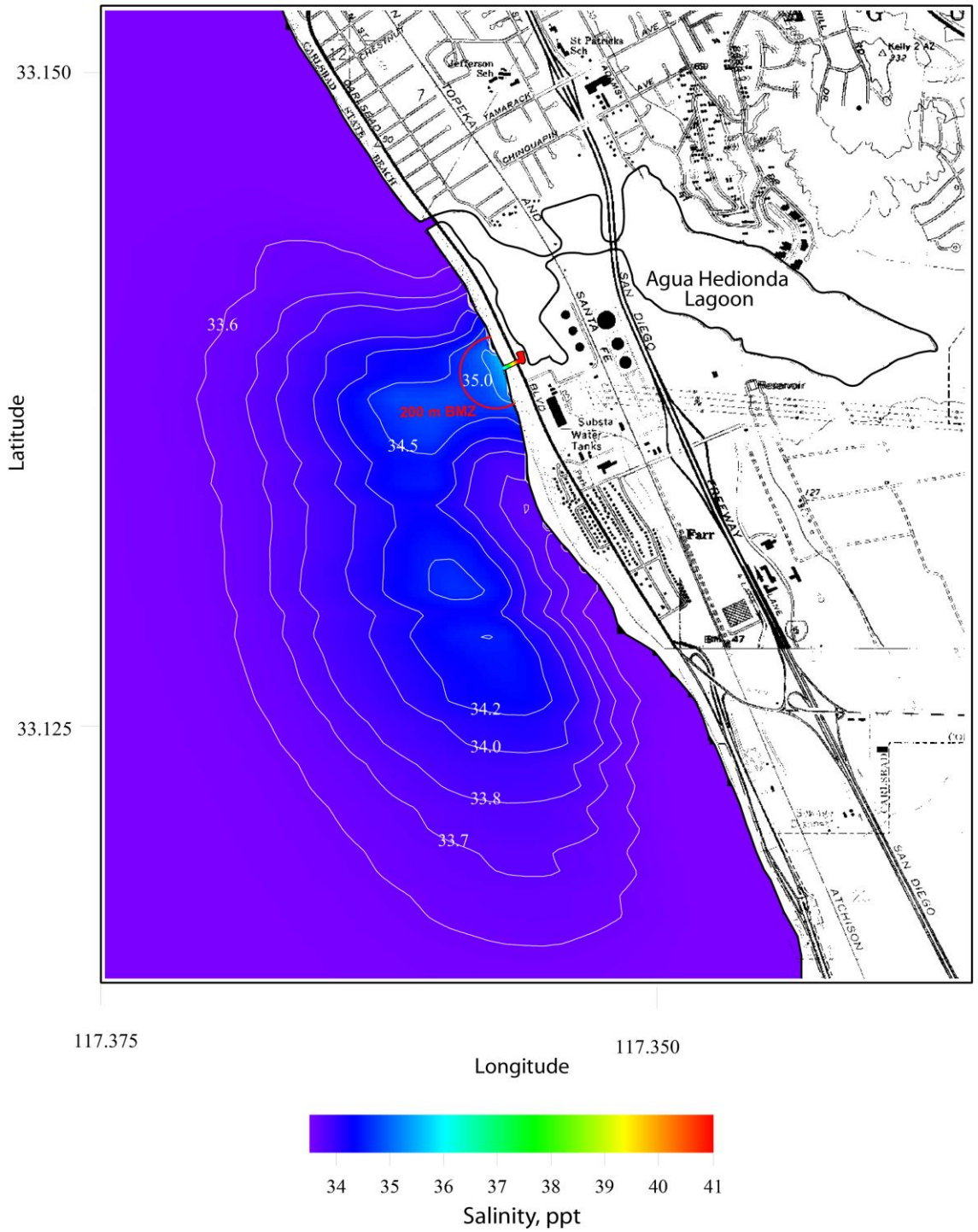

Figure 11: Bottom Salinity distribution time-averaged over proxy average-case 24 hour conditions (23 May 1994) for the 60 mgd upgrade of the Carlsbad Desalination Project. Total intake flow rate is 298 mgd, of which 178 mgd is flow augmentation for in-plant dilution. Product water production = 60 mgd. Total discharge = 238 mgd at 42 ppt. Salinity contoured in ppt with ambient ocean salinity = 33.52 ppt. BMZ with 200m radius shown in red. Frequency of recurrence = 50.01 %.

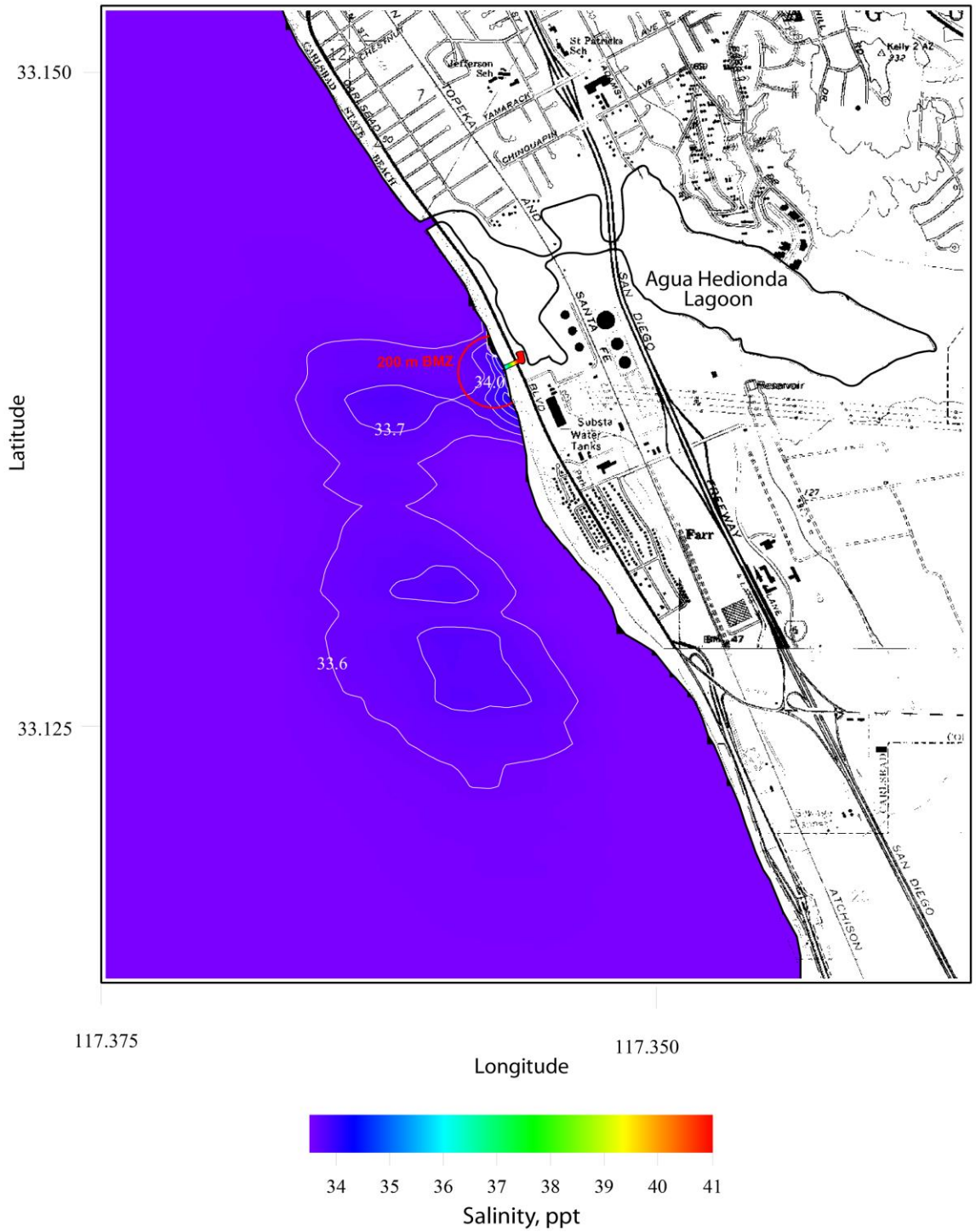

Figure 12: Depth-averaged water column salinity distribution time-averaged over proxy average-case 24 hour conditions (23 May 1994) for the 60 mgd upgrade of the Carlsbad Desalination Project. Total intake flow rate is 298 mgd, of which 178 mgd is flow augmentation for in-plant dilution. Product water production = 60 mgd. Total discharge = 238 mgd at 42 ppt. Salinity contoured in ppt with ambient ocean salinity = 33.52 ppt. BMZ with 200m radius shown in red. Frequency of recurrence = 50.01 %.

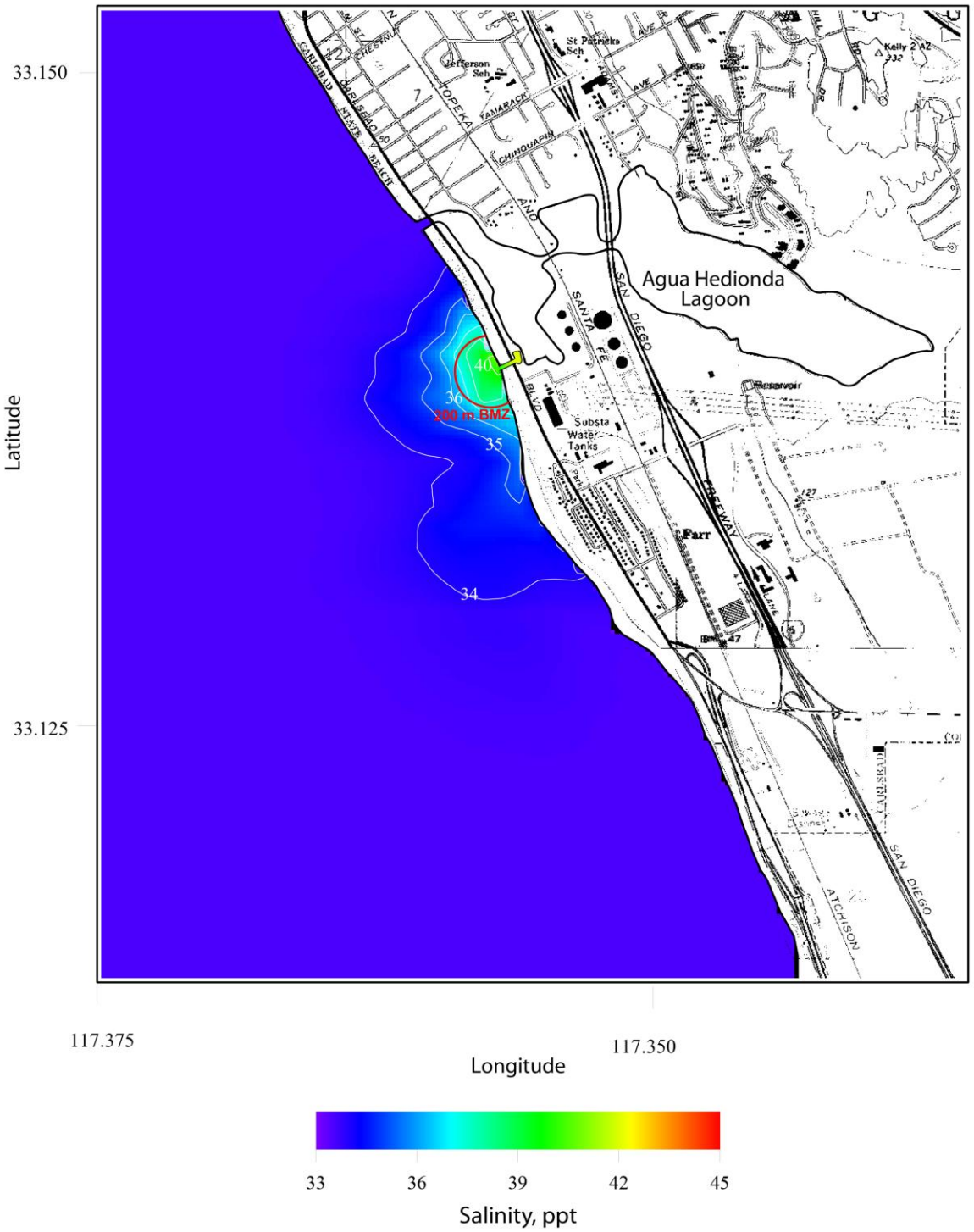

Figure 13: Bottom Salinity distribution time-averaged over proxy worst-case 24 hour conditions (17 August 1992) for the 60 mgd upgrade of the Carlsbad Desalination Project. Total intake flow rate is 298 mgd, of which 178 mgd is flow augmentation for in-plant dilution. Product water production = 60 mgd. Total discharge = 238 mgd at 42 ppt. Salinity contoured in ppt with ambient ocean salinity = 33.51 ppt. BMZ with 200m radius shown in red. Frequency of recurrence = 0.01 %.

(10 acres of sandy soft-bottom habitat), of the 200 m radius BMZ with bottom salinity in the range of 38 ppt to 40 ppt. At most points along 200 m radius BMZ boundary maximum salinity is 36.5 ppt. Because of the strong stratification of the brine plume and weak surf zone turbulence, brine salinity in the water column, (Figure 14), is substantially less than on the seabed. Figure 14 shows that maximum depth-averaged salinities reach 37 ppt directly seaward of the mouth of the discharge channel and decline to only 35.5 ppt along the 200 m BMZ boundary under worst-case daily-ocean mixing and advections conditions. Thus the discharge limits of the newly amended Ocean Plan are satisfied in the water column, but only marginally fulfilled on the seabed under the condition that the historic maximum observed salinity can be used as a measure of natural background salinity. However, it should be noted that the worst case outcome in figures 13 and 14 is a 1 in 7,500 event, with a recurrence probability of only 0.01%. Therefore, this marginal compliance outcome is not persistent and likely not repeatable; and the chances of periodic monitoring actually measuring such a worst case event day are extremely remote.

4.3 Long-term Dilution Results and Discharge Compliance Analysis

Figure 15 calculates the probability density function (histogram) for the discharge salinity at 200 m from the discharge point (green and red) for all 7,523 modeled outcomes from the time-stepped progression through the 20.5 year long record of boundary conditions and forcing functions plotted in Figures 7 and 8. During these time-stepped dilution simulations, the bottom bathymetry continuously varied based on equilibrium beach profile corrections to the 1998 SDG&E beach surveys. These beach profile corrections were calculated from the elliptic cycloid algorithms of the CEM (APPENDIX II) using wave height inputs from Figure 8 and beach fill history for Agua Hedionda Lagoon dredge disposal as listed in APPENDIX III.

For comparison, the probability density function for the daily ambient ocean salinity from Figure 9 is under-laid in transparent light blue in Figure 15 while the probability density function for the regulatory standard of 2 ppt over daily ambient ocean salinity is overlaid. All of the discharge outcomes where salinity at the 200 m BMZ falls between the probability distributions for ambient salinity and ambient + 2 ppt are shown in green because these represent outcomes in compliance with the new Ocean Plan discharge limit. The minimum brine salinity at the 200 m BMZ boundary that was calculated from these 20.5 year long dilution simulations is 32.8 ppt, corresponding to event days with minimum ocean salinity of 31.1 ppt. The median dilution result throughout the 20 year period of record gives an average brine salinity of 35.0 ppt in the plume at 200 m from the point of discharge. Altogether, 98 % of the 7,523 modeled outcomes produced discharge salinity that was less than or equal to 2 ppt above ambient ocean salinity at every point along the 200 m radius BZM semi-circle. Note, those outcomes where discharge salinity equaled ambient + 2ppt are hidden behind the dark blue histogram bars in Figure 15, but for clarity are plotted over the dark blue histogram bars in Figure 16; otherwise Figures 15 and 16 are identical. Outcomes where discharge salinity exceeded 2 ppt above daily ambient ocean salinity are the red "outlier" histogram bars that extend to the left of the dark blue histogram bars in Figure 15. These represent potential exceedances of the new Ocean Plan discharge limit, but are extremely rare and never persistent, accounting for only 2 % of the potential discharge cases over a 20.5 year period. Maximum brine salinity at 200 m from the point of discharge is 36.5 ppt, which has a probability of recurrence of only 0.01%, corresponding to ocean mixing conditions of the

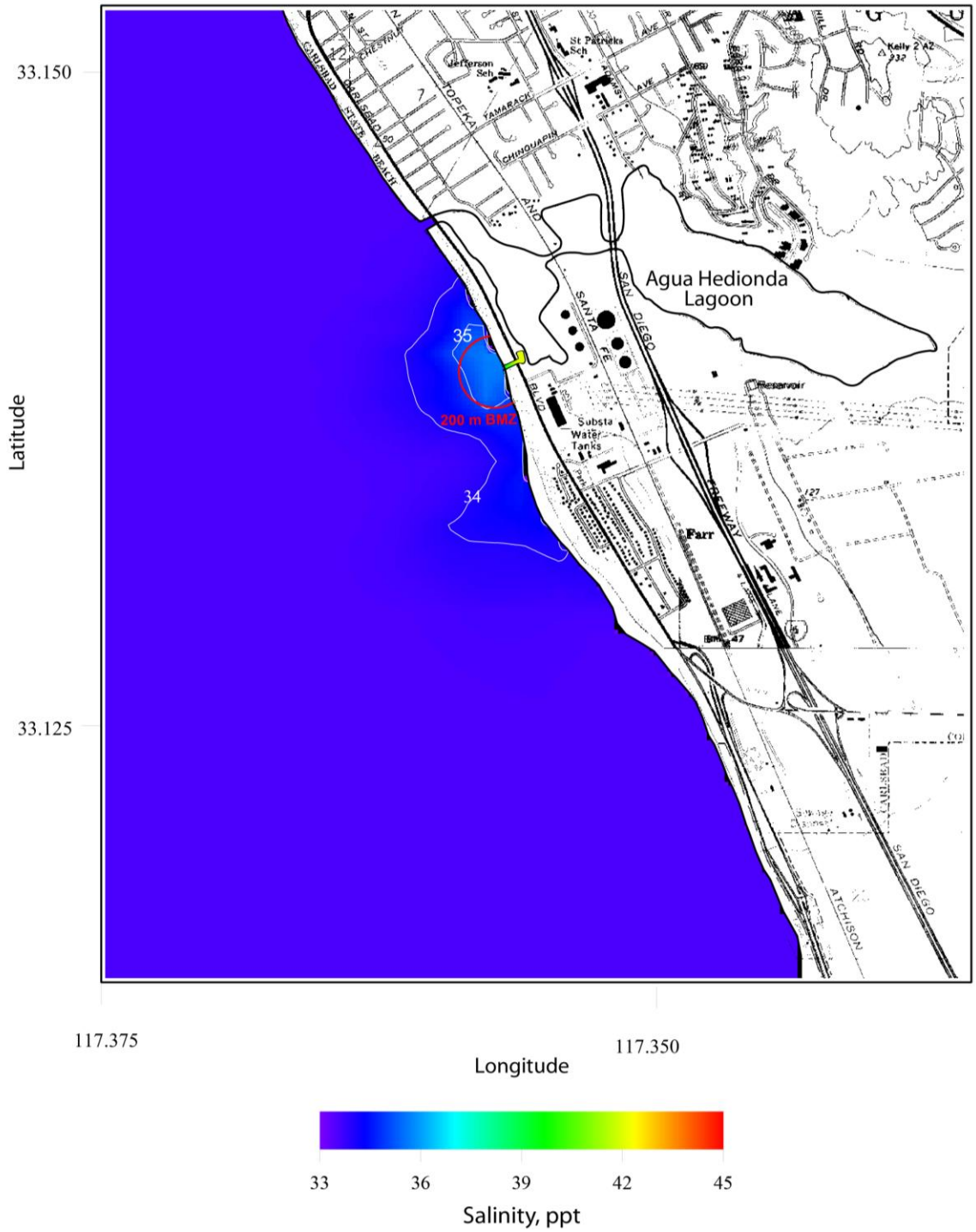

Figure 14: Depth-averaged water column salinity distribution time-averaged over proxy worst-case 24 hour conditions (August 1992) for the 60 mgd upgrade of the Carlsbad Desalination Project. Total intake flow rate is 298 mgd, of which 178 mgd is flow augmentation for in-plant dilution. Product water production = 60 mgd. Total discharge = 238 mgd at 42 ppt. Salinity contoured in ppt with ambient ocean salinity = 33.51 ppt. BMZ with 200m radius shown in red. Frequency of recurrence = 0.01 %.

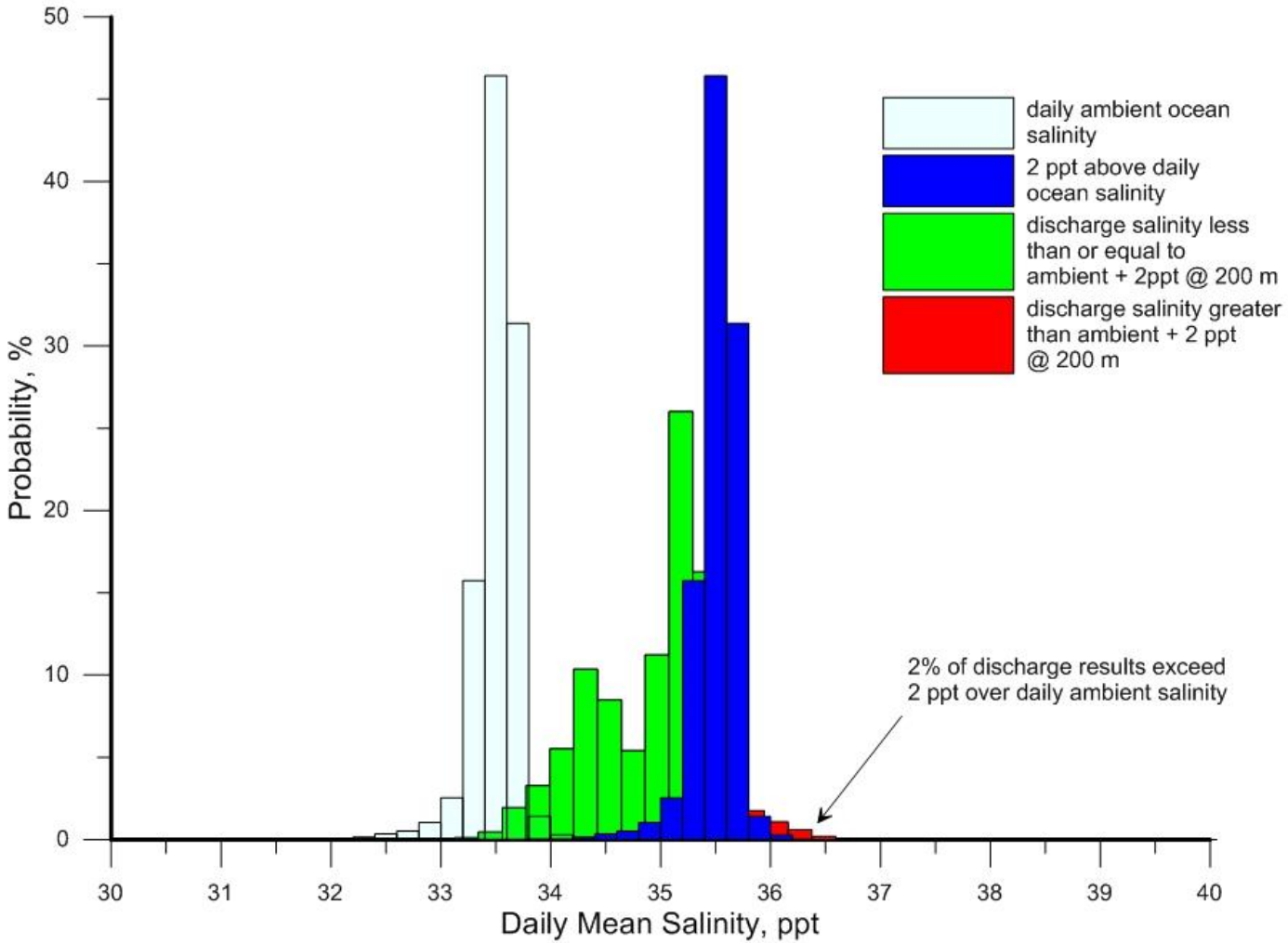

Figure 15. Probability density functions (histograms) for daily ocean salinity (light blue) and 2 ppt above daily ocean salinity (dark blue) vs discharge salinity on the sea bed at 200 m from the discharge point from the Carlsbad Desalination Project (green and red). Discharge results in green represent daily outcomes that were less than or equal to ambient salinity + 2ppt; while results in red represent daily outcomes that were greater than ambient salinity + 2ppt. Model results based on discharges of 238 mgd of concentrated seawater discharge at 42 ppt salinity.

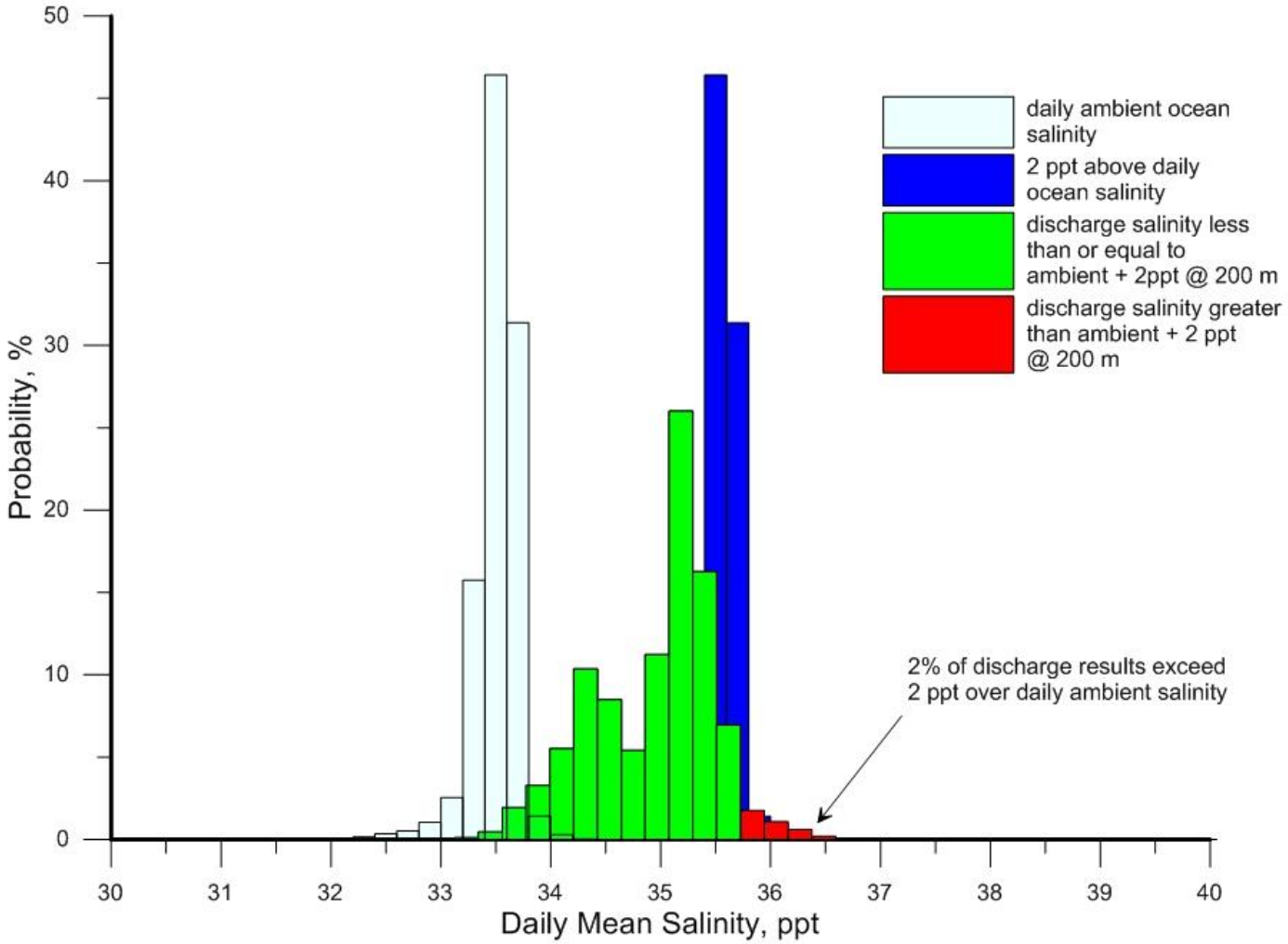

Figure 16. Probability density functions (histograms) for daily ocean salinity (light blue) and 2 ppt above daily ocean salinity (dark blue) vs discharge salinity on the sea bed at 200 m from the discharge point from the Carlsbad Desalination Project (green and red). Discharge results in green represent daily outcomes that were less than or equal to ambient salinity + 2ppt; while results in red represent daily outcomes that were greater than ambient salinity + 2ppt. Model results based on discharges of 238 mgd of concentrated seawater discharge at 42 ppt salinity.

worst-case day of 17 August 1992. No modeled outcomes exceed 36.3 ppt (the upper limit of natural ocean variability) by more than measurement error, which is generally regarded as +/- 0.2 ppt using standard temperature/conductivity probes for determination of practical salinity units (psu).

5) Exposure Time of Drifting Marine Organisms

Hyper-salinity sub-lethal impacts to marine organisms are not only a function of the incremental increase in salinity over natural background, but also the amount of time of exposure to that incremental increase. With the layout of the Carlsbad Desalination Project, exposure occurs during two separate dilution stages: 1) the in-plant dilution stage where ichthyoplankton (typically comprised of holoplankton, neroplankton, eggs and larvae) entrained in the discharge flow augmentation are blended with the raw brine (at 67 ppt) from the reverse osmosis process, and 2) the receiving water dilution phase where the partially diluted brine (typically 42 ppt) is mixed with the surfzone and nearshore water mass. In the following analysis, exposure time is evaluated for three separate 60 mgd production scenarios where the partially diluted brine can be 44 ppt, 42 ppt or 40 ppt.

5.1 Exposure Time During In-Plant Dilution: In-plant dilution occurs in a 400 ft. long dilution channel that measures 15 ft. wide and 8 ft. deep and empties into a dilution pond prior to discharge to the ocean through the discharge jetties, (cf. Figure 2). Exposure time is strictly limited by the travel time of the discharge stream in this channel, which in turn is controlled by the discharge flow rate of the partially diluted brine through the 8 ft x 15 ft. channel cross section. Table 1 below summarizes the key flow rate variables that control ichthyoplankton exposure time during the in-plant dilution stage.

Table 1: Exposure Time During In-Plant Dilution Stage

Intake Flow Rate (mgd)	Brine Discharge Rate from R.O. (mgd)	Discharge Salinity From R.O. (ppt)	Discharge Flow Augmentation (mgd)	Total Discharge Flow Rate (mgd)	Salinity in Discharge Channel (ppt)	Dilution Channel Exposure Time (min)
120	60	67	124	184	44.4	2.8
120	60	67	178	238	42	2.2
120	60	67	244	304	40.1	1.7

5.2 Exposure Time During Receiving Water Dilution: Ichthyoplankton drifting in the surfzone and nearshore currents are carried through the discharge plume along trajectories governed by the *Lagrangian drift* (Batchelor, 1970). The Lagrangian drift is the mean motion that would be observed by following that particle along its drift trajectory. The concept of Lagrangian mean motion is particularly important in the problem at hand because the water velocity in and around the plume varies from point to point due to the cross shore variation in the wave and tidal currents and the local velocity variation due to the discharge stream ejected from

the discharge jetties. Such variations in the local velocity field are referred to as *velocity gradients*, and those gradients govern the *Lagrangian drift* of a tiny marine organism according to:

$$\overline{U} = u\,(x_0,t) + \left\{ \left(\int_{t_0}^{t} u\,dt \right) \bullet \nabla u\,(x,t) \right\}_{x=x_0} \qquad (1)$$

Where $u(x_0,t)$ is the Eulerian velocity at a fixed point x_0 and at time t and ∇u is the velocity gradient. These velocities and velocity gradients were resolved by the SEDXPORT model over the entire nearshore domain by the wave and current algorithms described APPENDIX-II. The drift rates of organisms passing through these velocity gradients are not the same as the mean current speed measured by a fixed current meter located at a fixed point. The current meter will have an error in drift rate estimates due to the effects of velocity gradients acting on the organism at places away from the current meter location. A hydrodynamic model can correct for such errors because it can reconstruct the entire velocity gradient structure that is required to calculate the actual drift rate of a particle moving in a variable velocity field using equation (1). The drift rate of an organism passing through the discharge plume is calculated under the assumption that the organism is represented by a neutrally buoyant particle.

The exposure times to elevated salinity for organisms entrained in the discharge are plotted in Figure 17 for average-case conditions as detailed in Section 4.2 above. The travel time from the outlet of the discharge pond to a salinity in the range of 2 ppt over the natural background salinity will be limited to 26.9 minutes for discharges of 42 ppt at 238 mgd; increasing to 30.0 minutes for discharges of 44.4 ppt at 184 mgd; or declining to 24.3 minutes for discharges of 40.1 ppt at 304 mgd. The total amount of time the entrained organisms would be exposed to salinity in excess of 33.51 ppt (average natural background salinity) is 51.4 minutes for discharges of 42 ppt at 238 mgd; increasing to 56.7 minutes for discharges of 44.4 ppt at 184 mgd; or declining to 46.5 minutes for discharges of 40.1 ppt at 304 mgd. Regardless, such exposure durations at these worst-case brine plume salinity levels remain well below any known chronic toxicity thresholds for the relevant marine species of the Southern California Bight, (Graham, 2004; Weston, 2013; Voorhees et al., 2013).

6) Minimum Month Initial Dilution

6.1) Determination of Minimum Month Initial Dilution. The Ocean Plan establishes receiving water concentration standards that are to be achieved upon completion of initial dilution. Provision III.C.4.d of the Ocean Plan states:

For the purpose of this Plan, minimum initial dilution is the lowest average initial dilution within any single month of the year. Dilution estimates shall be based on observed waste characteristics, observed receiving water density structure, and the assumption that no currents, of sufficient strength to influence the initial dilution process, flow across the discharge structure.

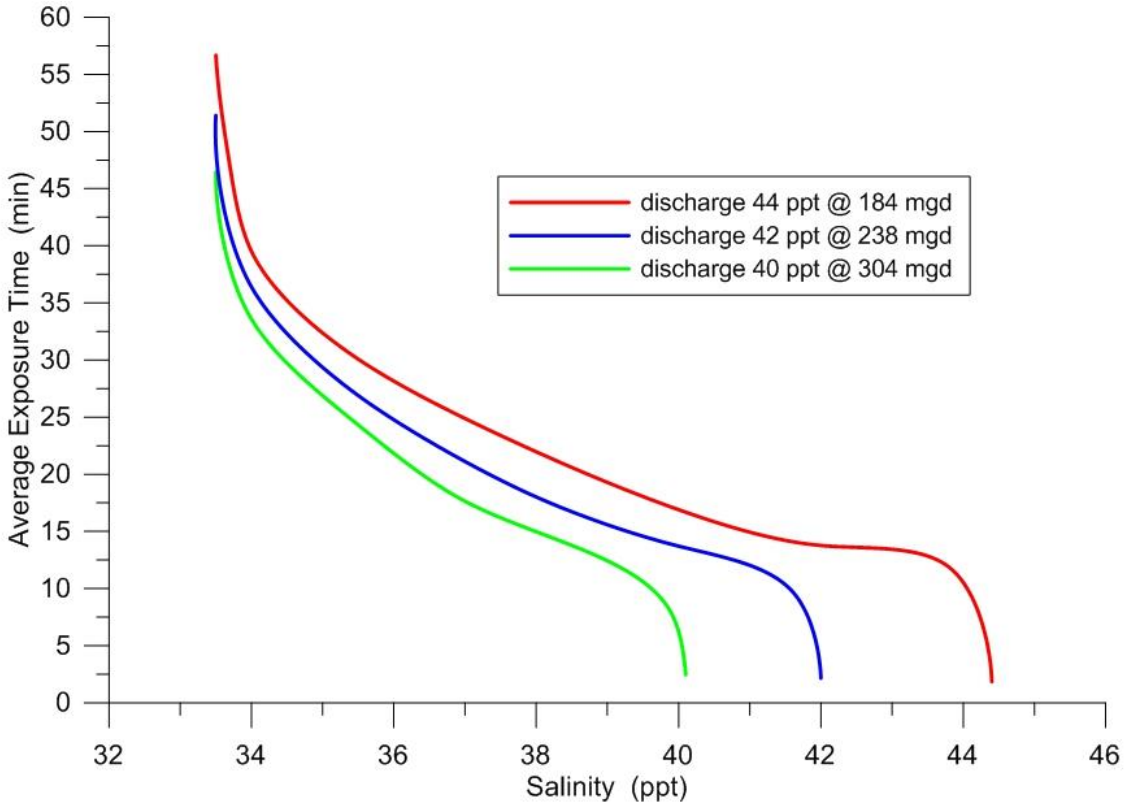

Figure 17. Average exposure times of organisms entrained in the discharge to elevated salinity from the outlet of the discharge pond for average case mixing conditions and three possible discharge scenarios at 60 mgd production rate. Average natural background salinity = 33.5 ppt.

Provision III.M.3.b of the 2015 Ocean Plan amendments requires owners or operators of desalination facilities to develop a dilution factor (Dm) for application to the BMZ:

> *The dilution factor (Dm) shall be developed within the Brine Mixing Zone using applicable water quality models that have been approved by the regional water boards in consultation with State Water Board staff.*

Worst case initial dilution for the CDP surface discharge would occur during periods when receiving water salinity and temperature are highest at the same time that wind, waves, currents, and ocean water levels are minimal. For purposes of identifying minimum month initial dilution within the 200-meter CDP brine mixing zone (BMZ), the SEDXPORT surfzone dilution model was used to superimpose the 60 mgd CDP discharge on a 20.5 year record of hydrodynamic drivers, including: wave, wind, current, ocean water levels, temperature. Based on the 20.5 year hydrodynamic record, worst case month initial dilution conditions were identified as having occurred in August 1992 (cf. Figures 7 & 8). The August 1992 conditions meet the criteria (worst case monthly dilution out of a 20.5 year record and minimal to near-zero ocean currents) established in Ocean Plan Provisions III.C.4.d for the determination of minimum initial dilution within the BMZ.

Figure 18 presents a probability histogram of computed initial dilution achieved at a 200 meter distance from the discharge jetty (e.g. the edge of the BMZ) for a 60 mgd CDP discharge under permanent stand-alone operation during the August 1992 worst case hydrodynamic conditions. These initial dilution results are evaluated at the seabed where the salinity of the partially diluted dense brine discharge is greatest. Initial dilutions during this worse case month (computed using six-hour time increments during the 31-day period) ranged from a low of 9.1:1 to a high of 17.3:1. Mean monthly dilution during this worst case month was $< Dm >$ = 10.4:1.

While instantaneous initial dilutions at any given point and any given time along the BMZ edge continuously vary with the instantaneous breaking wave heights, (whereby the surf zone mixing creates a natural diffuser), the 10.4:1 mean initial dilution at the 200 meter distance during August 1992 worst case conditions (probability of occurrence of 0.4 percent) represents the most conservative characterization of Ocean Plan-defined lowest initial dilution within any single month of the year to serve as the minimum initial dilution for the CDP discharge.

6.2 Implications on Receiving Water Compliance. Equation 1 of the 2015 Ocean Plan amendments establishes how the minimum month initial dilution is applied for purposes of determining effluent concentration standards required to implement the Ocean Plan receiving water salinity standard:

$$Ce = (2.0\,ppt + Cs) + Dm \times 2.0\,ppt \qquad \text{(Equation 1 of California Ocean Plan Amendment)}$$

where: Ce = the effluent concentration limit required to implement the Ocean Plan standard that receiving water salinity not exceed 2 ppt above ambient beyond the BMZ,

Cs = the natural background salinity, and

Dm = the minimum probable initial dilution expressed as parts of seawater per part brine discharge at the edge of the BMZ.

Applying a natural background salinity (Cs) of 33.5 ppt and a minimum initial dilution (Dm) of 10.4 to Equation 1, an effluent concentration standard (Ce) at M-002 as high a 56.3 ppt would satisfy compliance with the 2 ppt above ambient standard at the edge of the BMZ. Stated another way, a minimum month initial dilution (Dm) of only 3.25:1 would be required to ensure that a 42 ppt effluent concentration (Ce) at M-002 complies with the Ocean Plan receiving water standard that salinity not exceed 2 ppt above ambient beyond the BMZ. Since the minimum month initial dilution is projected to significantly exceed 3.25:1 for the 60 mgd CDP discharge, it can be seen that the proposed 42 ppt effluent concentration salinity standard (Ce) proposed by Poseidon Water LLC will achieve compliance with the 2 ppt above ambient Ocean Plan standard by a significant margin under minimum month conditions. Thus, while hydrodynamic modeling of the CDP discharge (see Figures 13, 15, and 16) shows a small probability (up to 2 percent) that the 2 ppt above ambient standard may be exceeded under short-term (6-hour or daily) periods, compliance with the Ocean Plan receiving water standard under minimum month conditions is assured.

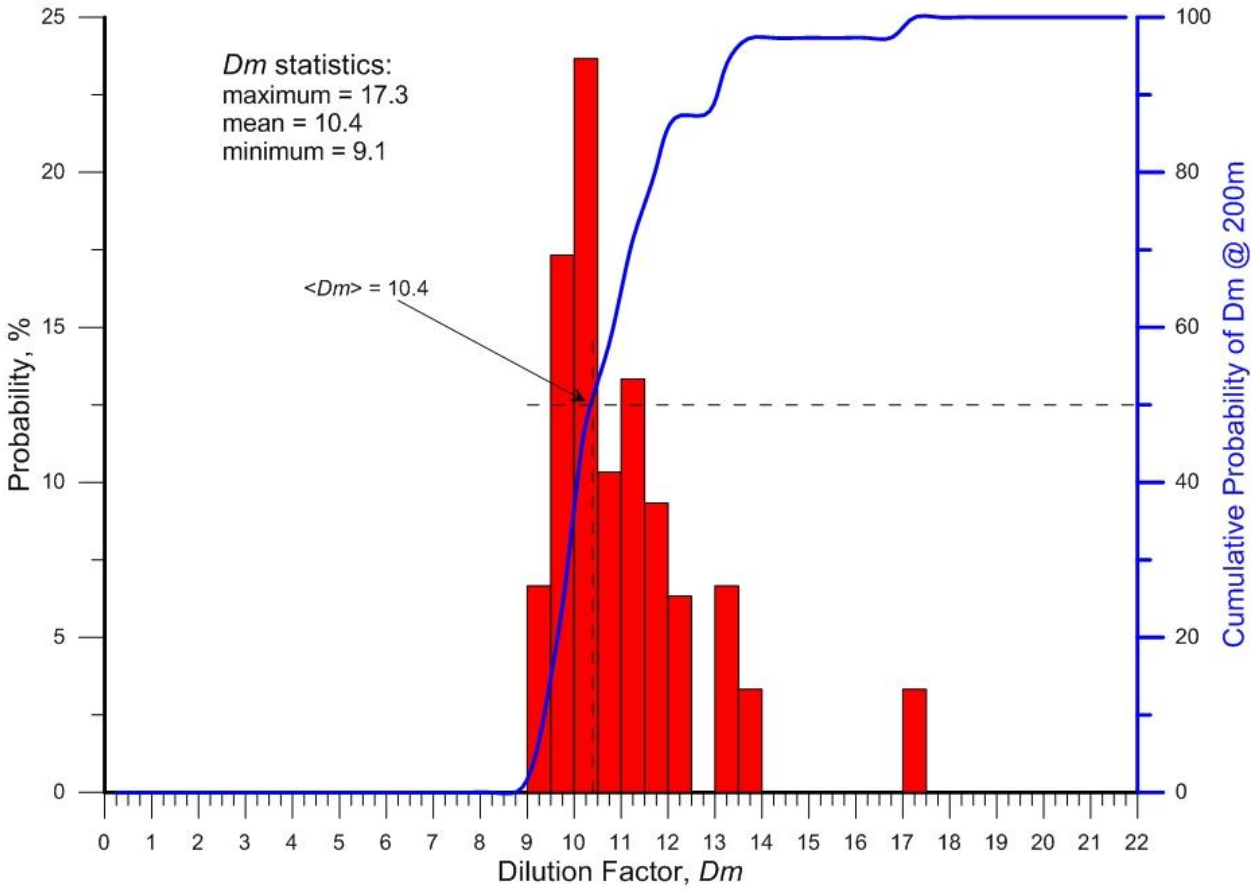

Figure 18. Computed initial dilution at a 200 meter discharge from the CDP discharge jetty under August 1992 hydrodynamic conditions for a 60 mgd CDP discharge under permanent stand-alone operations. Initial dilutions computed using six-hour time increments over the 31-day worst case month period. Average ambient receiving water salinity during the worst case month was 33.49, approximately the same as the long-term average.

7) Conclusions:

We present a hydrodynamic dilution analysis related to a potential increase in product water production for the Carlsbad Desalination Project (CDP) in the light of recent amendments to the California Ocean Plan. The proposed increase in production capacity of Carlsbad Desalination Project (presently under construction at about a stage of 90% completion) would be from 50 millions gallons per day (mgd) to 60 mgd. With this increase, we examine potential compliance with a new numeric water quality objective that limits brine discharges from ocean desalination plants (whose construction are 80% complete) to no more than 2 ppt over ambient ocean salinity (*natural background salinity*) at the outer edge of a *Brine Mixing Zone* (BMZ) measuring 200 m (656 ft) in radius around the point of discharge into the receiving waters. Under this new Ocean Plan amendment, *natural background salinity* is to be determined from 20 years of ocean salinity measurements representative of the at project site.

The dilution analysis uses a process-based dilution modeling system known as *SEDXPORT* applied to a brine discharge scenario of 238 mgd of unheated brine discharged at 42 ppt salinity from the existing discharge channel at Encina Power Station, Carlsbad, CA. The EPA certified dilution models CORMIX and Visual Plumes do not contain the physics for nearshore or surf zone mixing and transport as occurs with discharges from the Encina Power Station and from the Carlsbad Desalination Project. SEDXPORT is the only available model that accounts for these coastal processes, and is the only model approved by the California State Water Resources Control Board for modeling dilution of storm drain runoff into the nearshore, (SCCWRP, 2012). Because surf zone water depths at this site constantly fluctuate due to seasonal beach profile changes and bi-annual beach disposal from Agua Hedionda Lagoon maintenance dredging, time varying bathymetry was applied to the dilution analysis based on published peer-reviewed algorithms that have been coded into the Coastal Evolution Model (CEM). Twenty year-long records of waves, currents, winds, ocean salinity and temperature were used to initialize and drive these models to produce 7,523 modeled outcomes for brine dispersion and dilution evaluated on the boundaries of a 200 m radius BMZ.

The minimum brine salinity at the 200 m BMZ boundary that was calculated from these 20.5 year-long dilution simulations is 32.8 ppt, corresponding to event days with minimum ocean salinity of 31.1 ppt. The median dilution result throughout the 20.5 year period of record gives an average brine salinity of 35.0 ppt in the plume at 200 m from the point of discharge. Altogether, 98 % of the 7,523 modeled outcomes produced discharge salinity that was less than or equal to 2 ppt above ambient ocean salinity at every point along the 200 m radius BMZ. The travel time for organisms entrained in the discharge from the outlet of the discharge pond to the point where the salinity is no greater than 2 ppt or greater over the natural background salinity is generally limited to 27 minutes. Outcomes where discharge salinity exceeded 2 ppt above daily ambient ocean salinity are extremely rare and never persistent, accounting for only 2 % of the potential discharge cases over a 20.5 year period. No modeled outcomes exceed 36.3 ppt (the upper limit of natural ocean variability) by more than measurement error, which is generally regarded as +/- 0.2 ppt using standard temperature/conductivity probes for determination of practical salinity units (psu). While hydrodynamic modeling of the CDP discharge (see Figures 13, 15, and 16) shows a small probability (up to 2 percent) that the 2 ppt above ambient standard may be exceeded under short-term (6-hour or daily) periods, compliance with the Ocean Plan receiving water standard under minimum month conditions is assured.

8) References:

Batchelor, G. K., 1970, *An Introduction to Fluid Mechanics*, Cambridge Univ. Press, New York., 615 pp.

CalCOFI, 2014, "California Cooperative Oceanic Fisheries Investigation", Southern California Coastal Ocean Observation System, SCOOS Data: http://www.calcofi.org/data/sccoos/sccoos-data.html

CalTrans, 2015, "Coastal Project Design Storm Guidance and Wave Run-up Analysis," State Agreement 53A0184, Task Order Number 03, State of California, Department of Transportation Department Task Manager: Bruce Swanger, P.E.

CDIP (2012), "Coastal data information program," *SIO Reference Series*, 01-20 and http://cdip.ucsd.edu.

EIR, 2005 "Precise Development Plan and Desalination Plant," EIR 03-05-Sch #2004041081, prepared for City of Carlsbad by Dudek and Associates, December, 2005.

Graham, J. B., 2004, "Marine biological considerations related to the reverse osmosis desalination project at the Applied Energy Sources, Huntington Beach Generating Station," Appendix-S in REIR, 2005, 100 pp.

Inman, D. L., M. H. S. Elwany & S. A. Jenkins, 1993, "Shoreline and bar-berm profiles on ocean beaches," *Jour. Geophys. Res.*, v. 98, n. C10, p. 18,181–18,199.

Jenkins, S. A. and J. Wasyl, 2005, "Hydrodynamic Modeling of Dispersion and Dilution of Concentrated Seawater Produced by the Ocean Desalination Project at the Encina Power Plant, Carlsbad, CA, Part II: Saline Anomalies due to Theoretical Extreme Case Hydraulic Scenarios," submitted to Poseidon Resources, 97pp.

Jenkins, S. A. and J. Wasyl, 2005, "Coastal evolution model," Scripps Institution of Oceanography Tech Report No. 58, 179 pp + appendices. http://repositories.cdlib.org/sio/techreport/58/

Jenkins, S. A. and D. L. Inman, 2006, "Thermodynamic solutions for equilibrium beach profiles", *Jour. Geophys. Res.*, v.3, C02003, doi:10.1029/2005JC002899, 2006. 21pp.

Jenkins, S. A., J. Paduan, P. Roberts, D. Schlenk, and J. Weis, 2012, "Management of Brine Discharges to Coastal Waters; Recommendations of a Science Advisory Panel", submitted at the request of the California Water Resources Control Board, 56 pp. + App.

Jenkins, S. A., 2013, "Technical Memorandum: Shoreline Evolution Analysis of Impacts Related to Removal of the South Beach Groin at Encina Power Station, Carlsbad," submitted to NRG Energy, 90 pp.

SCCWRP, 2012, Southern California Coastal Water Research Project: "Management of Brine Discharges to Coastal Waters - Recommendations of a Science Advisory Panel. Technical Report 694 to the State Water Resources Control Board, Southern California Coastal Water Research Project, Costa Mesa, CA.

SIO, 2013, "SIO shore station, Scripps Pier", http://www-mlrg.ucsd.edu/shoresta/mnSIOMain/siomain.htm

SWRCB, 2014, "DESALINATION FACILITY INTAKES, BRINE DISCHARGES, AND THE INCORPORATION OF OTHER NONSUBSTANTIVE CHANGES, Draft Staff Report Including the Draft Substitute Environmental Documentation Amendment to the Water Quality Control Plan For Ocean Waters of California, 206 pp.

Tenera, 2008, **"**Cabrillo Power I LLC, Encina Power Station 316(b) Cooling Water Intake Impingement Mortality and Entrainment Characterization Study: Effects on the Biological Resources of Agua Hedionda Lagoon and the Nearshore Ocean Environments" submitted to NRG Energy, 220 pp

USACE, 1993, "Existing State of San Diego County Coast," US Army Corps of Engineers, Los Angeles District, Tech Rpt 93-1, 335 pp.

Voorhees, J.P., B.M. Phillips, B.S. Anderson, K. Siegler, S. Katz, L. Jennings, R.S. Tjeerdema, J. Jensen, and M. de la Paz Capio-Obeso. 2013. Hypersalinity toxicity thresholds for nine California Ocean Plan toxicity test protocols. *Archives of Environmental Contamination and Toxicology* 65:665-670

Weston Solutions, (2013), "High-Salinity Sensitivity Study: Short- and Long-Term Exposure Assessments", submitted to West Basin Municipal Water District, 571 pp. http://www.waterboards.ca.gov/water_issues/programs/ocean/desalination/dos/sal study4wbmd.

APPENDIX-I: Technical Background on the SEDXPORT Dilution Modeling System:

The SEDXPORT modeling system has been extensively peer reviewed by 8 independent experts and can be found in the public records of the State Water Resources Control Board, the California Coastal Commission and the Cities of Carlsbad, Huntington Beach, Santa Cruz and Santa Barbara. SEDXPORT was also employed in the dilution studies for LADWP (Jenkins and Wasyl, 2005) and for West Basin's DDF (Jenkins and Wasyl, 2008b), and San Diego Diego County Water Authority (SDCWA, 2013). Formal peer review history of SEDXPORT includes:

1997- Reviewing Agency: State Water Resources Control Board
Project: NPDES 316 a/b Permit renewal, Encina Power Plant, Carlsbad, CA
Reviewer: Dr. Andrew Lissner, SAIC, La Jolla, CA

1998- Reviewing Agency: California Coastal Commission
Project: Coastal Development Permit, San Dieguito Lagoon Restoration
Reviewers: Prof. Ashish Mehta, University of Florida, Gainesville
Prof. Paul Komar, Oregon State University, Corvallis; Prof. Peter Goodwin, University of Idaho, Moscow

2000- Reviewing Agency: California Coastal Commission
Project: Coastal Development Permit, Crystal Cove Development
Reviewers: Prof. Robert Wiegel, University of California, Berkeley
Dr. Ron Noble, Noble Engineers, Irvine, CA

2002- Reviewing Agency: California Coastal Commission
Project: Coastal Development Permit, Dana Point Headland Reserve
Reviewers: Prof. Robert Wiegel, University of California, Berkeley ;
Dr. Richard Seymour, University of California, San Diego

2003- Reviewing Agency: City of Huntington Beach
Project: EIR Certification, Poseidon Desalination Project
Reviewer: Prof. Stanley Grant, University of California, Irvine

SEDXPORT was also reviewed by the California State Water Resources Control Board, and (SCCWRP, 2012) and by the City of San Diego.

SEDXPORT Architecture and Process Physics:

SEDXPORT modeling system has been built in a modular computational architecture (Figure Ia) which links together a series of process models referred to as modules (Jenkins and Wasyl, 2007). The modules are divided into two major clusters: 1) those which prescribe hydrodynamic forcing functions; and, 2) those which prescribe the mass sources acted upon by the hydrodynamic forcing to produce dispersion and transport. The cluster of modules for hydrodynamic forcing ultimately prescribes the velocities and diffusivities induced by wind, waves, and tidal flow for each depth increment at each node in the grid network.

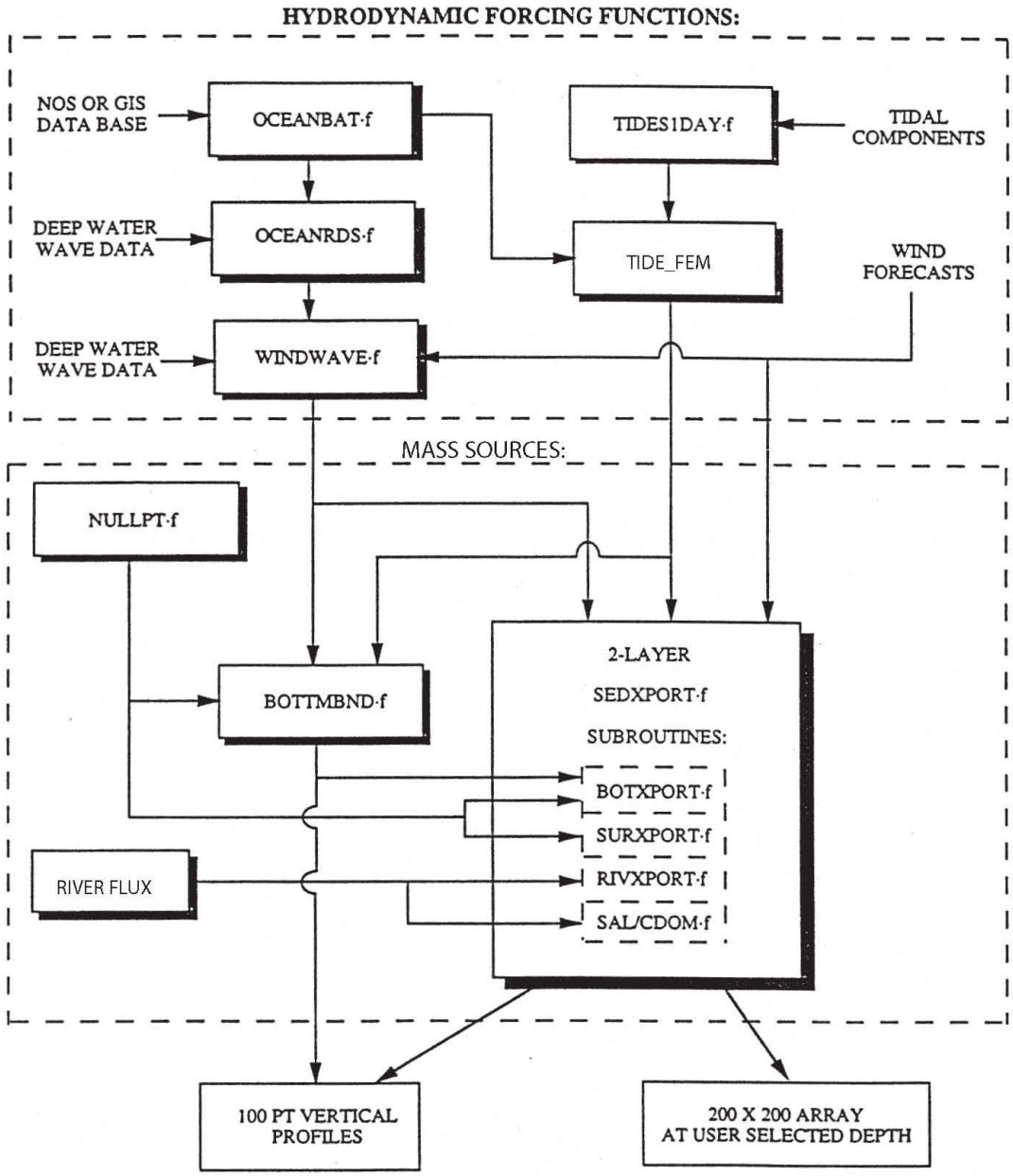

Figure Ia: Flow chart of the SEDXPORT farfield hydrodynamic model

The finite element current module, **TIDE_FEM**, (Jenkins and Wasyl, 1990; Inman and Jenkins, 1996) will be employed to evaluate the tidal currents at the project site. **TIDE_FEM** was built from some well-studied and proven computational methods and numerical architecture that have done well in predicting shallow water tidal propagation in Massachusetts Bay (Connor and Wang, 1974) and along the coast of Rhode Island, (Wang, 1975), and have been reviewed in basic text books (Weiyan, 1992) and symposia on the subject, e.g., Gallagher (1981). **TIDE_FEM** employs a variant of the vertically integrated equations for shallow water tidal propagation after Connor and Wang (1975). These are based upon the Boussinesq approximations with Chezy friction and Manning's roughness. The finite element discretization is based upon the commonly used Galerkin weighted residual method to specify integral functionals that are minimized in each finite element domain using a variational scheme, see Gallagher (1981). Time integration is based upon the simple trapezoidal rule (Gallagher, 1981).

The computational architecture of **TIDE_FEM** is adapted from Wang (1975), whereby a transformation from a **global** coordinate system to a **natural** coordinate system based on the unit triangle is used to reduce the weighted residuals to a set of order-one ordinary differential equations with constant coefficients. These coefficients (**influence coefficients**) are posed in terms of a **shape function** derived from the natural coordinates of each nodal point in the computational grid. The resulting systems of equations are assembled and coded as banded matrices and subsequently solved by **Cholesky's method**, see Oden and Oliveira (1973) and Boas (1966). The hydrodynamic forcing used by **TIDE_FEM** is based upon inputs of the tidal constituents derived from Fourier decomposition of tide gage records. Tidal constituents are input into the module **TID_DAYS**, which resides in the hydrodynamic forcing function cluster. **TID_DAYS** computes the distribution of sea surface elevation variations in Monterey Bay based on the tidal constituents derived from the tide gage station at Santa Barbara, NOAA #941-1340. Forcing for **TIDE_FEM** is applied by the distribution in sea surface elevation across the deep water boundary of the computational domain.

Wave driven currents will be calculated from wave measurements by the Coastal Data Information Program (CDIP) arrays and NOAA buoys. These measurements will be back refracted out to deep water to correct for propagation and shoaling effects between the monitoring sites and the project site. The waves were then forward refracted onshore to give the variation in wave heights, wave lengths and directions throughout the nearshore around the project site. The numerical refraction-diffraction code used for both the back refraction from these wave monitoring sites out to deep water, and the forward refraction to the project site is **OCEANRDS**. This code calculates the simultaneous refraction and diffraction patterns of the swell and wind wave components propagating over bathymetry replicated by the **OCEANBAT** code . OCEANBAT generates the associated depth fields for the computational grid networks of both **TID_FEM** and **OCEANRDS** using packed bathymetry data files derived from the National Ocean Survey (NOS) depth soundings compiled by GEODAS. The structured depth files written by **OCEANBAT** are then throughput to the module **OCEANRDS**, which performs a refraction-diffraction analysis from deep water wave statistics. **OCEANRDS** computes local wave heights, wave numbers, and directions for the swell component of a two-component, rectangular spectrum.

The wave data are throughput to a wave current algorithm in **SEDXPORT** which calculates the wave-driven longshore currents, $v(r)$. These currents were linearly superimposed on the tidal current. The wave-driven longshore velocity, $v(r)$, is determined from the longshore

current theories of Longuet-Higgins (1970). Once the tidal and wave driven currents are resolved by **TIDE_FEM** and **OCEANRDS**, the dilution and dispersion of brine and backwash constituents is computed by the stratified transport algorithms in SEDXPORT . The SEDXPORT code is a time stepped finite element module which solves the advection-diffusion equations over a fully configurable 3-dimensional grid. The vertical dimension is treated as a two-layer ocean, with a surface mixed layer and a bottom layer separated by a pycnocline interface. The code accepts any arbitrary density and velocity contrast between the mixed layer and bottom layer that satisfies the Richardson number stability criteria and composite Froude number condition of hydraulic state.

The SEDXPORT codes do not time split advection and diffusion calculations, and will compute additional advective field effects arising from spatial gradients in eddy diffusivity, (the so-called "gradient eddy diffusivity velocities" after Armi, 1979). Eddy mass diffusivities are calculated from momentum diffusivities by means of a series of Peclet number corrections based upon TSS and TDS mass and upon the mixing source. Peclet number corrections for the surface and bottom boundary layers are derived from the work of Stommel (1949) with modifications after Nielsen (1979), Jensen and Carlson (1976), and Jenkins and Wasyl (1990). Peclet number correction for the wind-induced mixed layer diffusivities are calculated from algorithms developed by Martin and Meiburg (1994), while Peclet number corrections to the interfacial shear at the pycnocline are derived from Lazara and Lasheras (1992a;1992b). The momentum diffusivities to which these Peclet number corrections are applied are due to Thorade (1914), Schmidt (1917), Durst (1924), and Newman (1952) for the wind-induced mixed layer turbulence and to Stommel (1949) and List, et al. (1990) for the current-induced turbulence.

SEDXPORT solves the eddy gradient form of the advection diffusion equation for the water column density field:

$$\frac{\partial \rho}{\partial t} = \left(\vec{u} \bullet \nabla \varepsilon\right) \bullet \nabla \rho - \varepsilon \nabla^2 \rho + \rho_0 Q_0 \qquad (1)$$

where $\vec{u}$ is the vector velocity from a linear combination of the wave and tidal currents, ε is the mass diffusivity, ∇ is the vector gradient operator and ρ is the water mass density in the nearshore dilution field; and ρ_0 is the density of the water discharged by the discharge at a flow rate $\frac{dV_0}{dt}$. The density of the discharge is a function of the bulk density of the suspended solids ρ_s and the density of the discharge fluid ρ_f that transports those solids, or:

$$\rho_0 = \rho_s + (1-N)\,\rho_f = \rho_q N + (1-N)\,\rho_f \qquad (2)$$

where N is the volume concentration of suspended solids equal to the ratio of suspended solids to sample volume; and ρ_q is the density of the suspended solid particles taken to be fine-grained quartz or ferric hydroxide floc.

Both the density of the receiving water ρ and the density of the discharge fluid ρ_f is a function of temperature, *T*, and salinity, *S*, according to the equation of state expressed in terms of the specific volume, $\alpha = 1/\rho$ and $\alpha_f = 1/\rho_f$ or:

$$\frac{d\alpha}{\alpha} = \frac{1}{\alpha}\frac{\partial \alpha}{\partial T}dT + \frac{1}{\alpha}\frac{\partial \alpha}{\partial S}dS \qquad (3)$$
$$\frac{d\alpha_f}{\alpha_f} = \frac{1}{\alpha_f}\frac{\partial \alpha_f}{\partial T}dT + \frac{1}{\alpha_f}\frac{\partial \alpha_f}{\partial S}dS$$

The factor $1/\alpha\,\partial\alpha/\partial T$, which multiplies the differential temperature changes, is known as the coefficient of thermal expansion and is typically 2 x 10^{-4} per ^{o}C for seawater; the factor $1/\alpha\,\partial\alpha/\partial S$, multiplying the differential salinity changes, is the coefficient of saline contraction and is typically 8 x 10^{-4} per part per thousand (ppt) where 1.0 ppt = 1.0 g/L of total dissolved solids (TDS). For a standard seawater, the specific volume has a value $\alpha = 1/\rho$ = 0.97264 cm^3/g. If the percent change in specific volume by equation (3) is less than zero, then the water mass is heavier than standard seawater, and lighter if the percent change is greater than zero. Solutions to the density field of the discharge plume from the outfall are calculated from equation (1) by **SEDXPORT,** from which computations of local discharge salinity and temperature, can be made using equation (3)

Solutions for the density and concentration fields calculated by the SEDXPORT codes from equations (1)-(3), are through put to the dilution codes of **MULTINODE** to resolve dilution factors according to (4) and (5). These codes solve for the dilution factor (mixing ratio) for each cell in the finite element mesh of the nearshore computational domain based on a mass balance between imported exported and resident mass of that cell. The diffusivity, ε, in (1) controls the strength of mixing and dilution of the seawater and storm water constituents in each cell and varies with position in the water column relative to the pycnocline interface. Vertical mixing includes two mixing mechanisms at depths above and below the pycnocline: 1) fossil turbulence from the bottom boundary layer, and 2) wind mixing in the surface mixed layer. The pycnocline depth is treated as a zone of hindered mixing and varies in response to the wind speed and duration. Below the pycnocline, only turbulence from the bottom wave/current boundary layer contributes to the local diffusivity. In the nearshore, breaking wave activity also contributes to mixing. The surf zone (zone of initial dilution) is treated as a line source of turbulent kinetic energy by the subroutine **SURXPORT**. This subroutine calculates seaward mixing from fossil surf zone turbulence, and seaward advection from rip currents embedded in the line source. Both the eddy diffusivity of the line source and the strength and position of the embedded rip currents are computed from the shoaling wave parameters evaluated at the breakpoint, as throughput of **OCEANRDS**.

APPENDIX-II: Coastal Evolution Model

The Coastal Evolution Model (CEM) is a process-based numerical model. It consists of a Littoral Cell Model (LCM) and a Bedrock Cutting Model (BCM), both coupled and operating in varying time and space domains (Figure A1) determined by sea level and the coastal boundaries of the littoral cell at that particular sea level and time. At any given sea level and time, the LCM accounts for erosion of uplands by rainfall and the transport of mobile sediment along the coast by waves and currents, while the BCM accounts for the cutting of bedrock by wave action in the absence of a sedimentary cover.

In both the LCM and BCM, the coastline of the littoral cell is divided into a series of coupled control cells (Figure A2). Figure A3 shows the arrangement of coupled control cells used to model the impacts of removal of the South Beach Groin. Each control cell is a small coastal unit of uniform geometry where a balance is obtained between shoreline change and the inputs and outputs of mass and momentum. The model sequentially integrates over the control cells in a down-drift direction so that the shoreline response of each cell is dependent on the exchanges of mass and momentum between cells, giving continuity of coastal form in the down-drift direction. Although the overall computational domain of the littoral cell remains constant throughout time, there is a different coastline position at each time step in sea level. For each coastline position there exists a similar set of coupled control cells that respond to forcing by waves and current. Time and space scales used for wave forcing and shoreline response (applied at 6 hour intervals) and sea level change (applied annually) are very different. To accommodate these different scales, the model uses multiple nesting in space and time, providing small length scales inside large, and short time scales repeated inside of long time scales.

The LCM (Figure 4, upper) has been used to predict the change in shoreline width and beach profile resulting from the longshore transport of sand by wave action where sand source is from river runoff or from tidal exchange at inlets (e.g., Jenkins and Inman, 1999). More recently it has been used to compute the sand level change (farfield effect) in the prediction of mine burial (Jenkins and Inman, 2002; Inman and Jenkins, 2002). Time-splitting logic and feedback loops for climate cycles and sea level change were added to the LCM together with long run time capability to give a numerically stable couple with the BCM.

In the LCM, the variation of the sediment cover with time is modeled by time-stepped solutions to the sediment continuity equation (otherwise known as the *sediment budget*) applied to the boundary conditions of the coupled control cell mesh diagramed schematically in Figure 3. The sediment continuity equation is written (Jenkins, et al, 2007):

$$\frac{\partial q}{\partial t} = \frac{\partial}{\partial y}\left(\varepsilon \frac{\partial q}{\partial y}\right) - V_l \frac{\partial q}{\partial y} + J(t) - R(t) \qquad (1)$$

Where q is the sediment volume per unit length of shoreline (m^3/m), ε is the mass diffusivity, V_l is the longshore current, *J(t)* is the flux of new sediment into the littoral cell from watrersheds and *R(t)* is the flux of sediment lost to sinks , typically submarine canyons, lagoons, spits, harbors or windblown losses. The first term in (1) is the surf diffusion while the second is divergence of drift. For any given control cell in Figure 10, (1) may be discretized in terms of the rate of change of beach volume, *V*, in time t, given by:

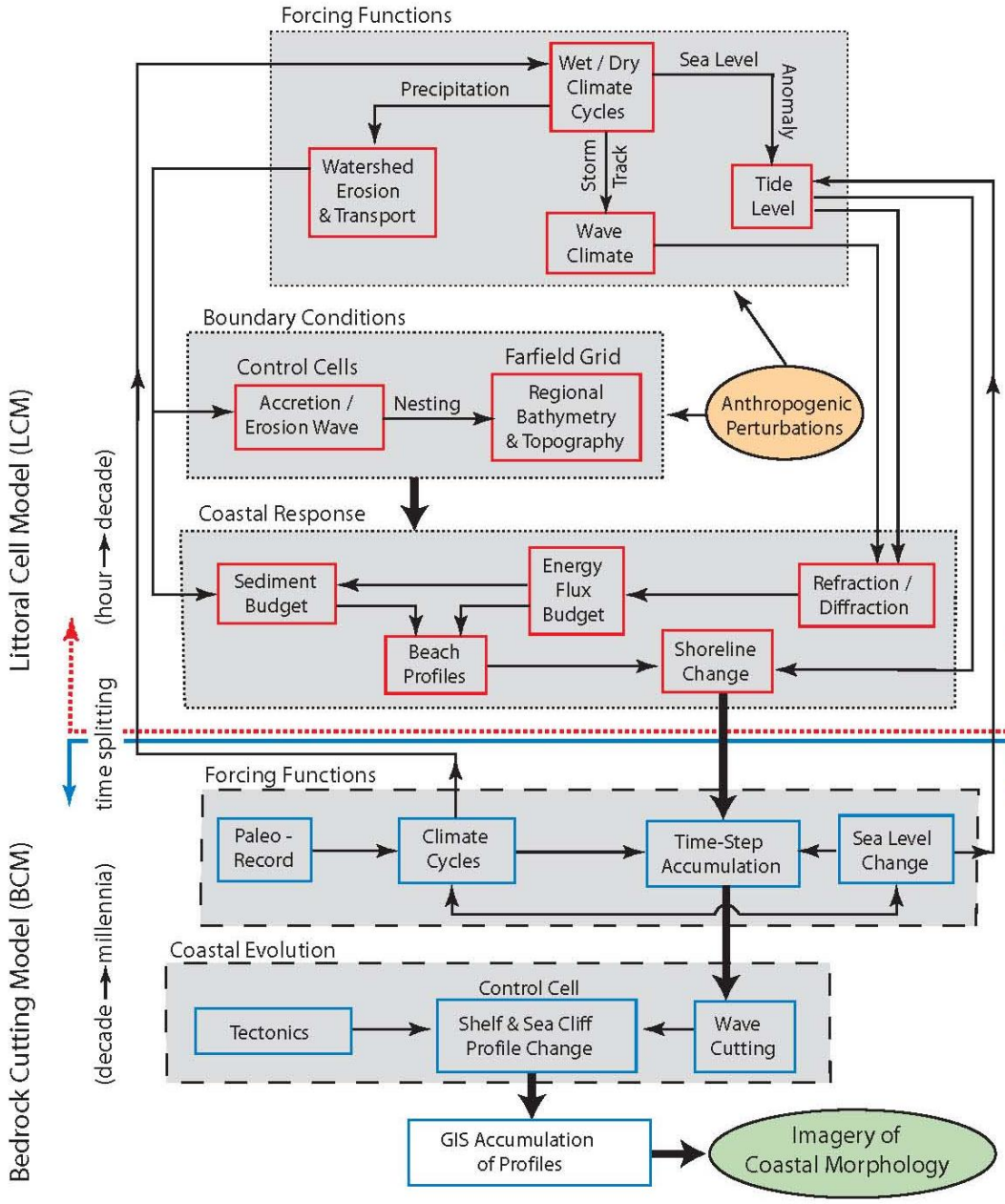

Figure A1: Architecture of the Coastal Evolution Model consisting of the Littoral Cell Model (above) and the Bedrock Cutting Model (below). Modules (shaded) are formed of coupled primitive process models. (from Jenkins and Wasly, 2005).

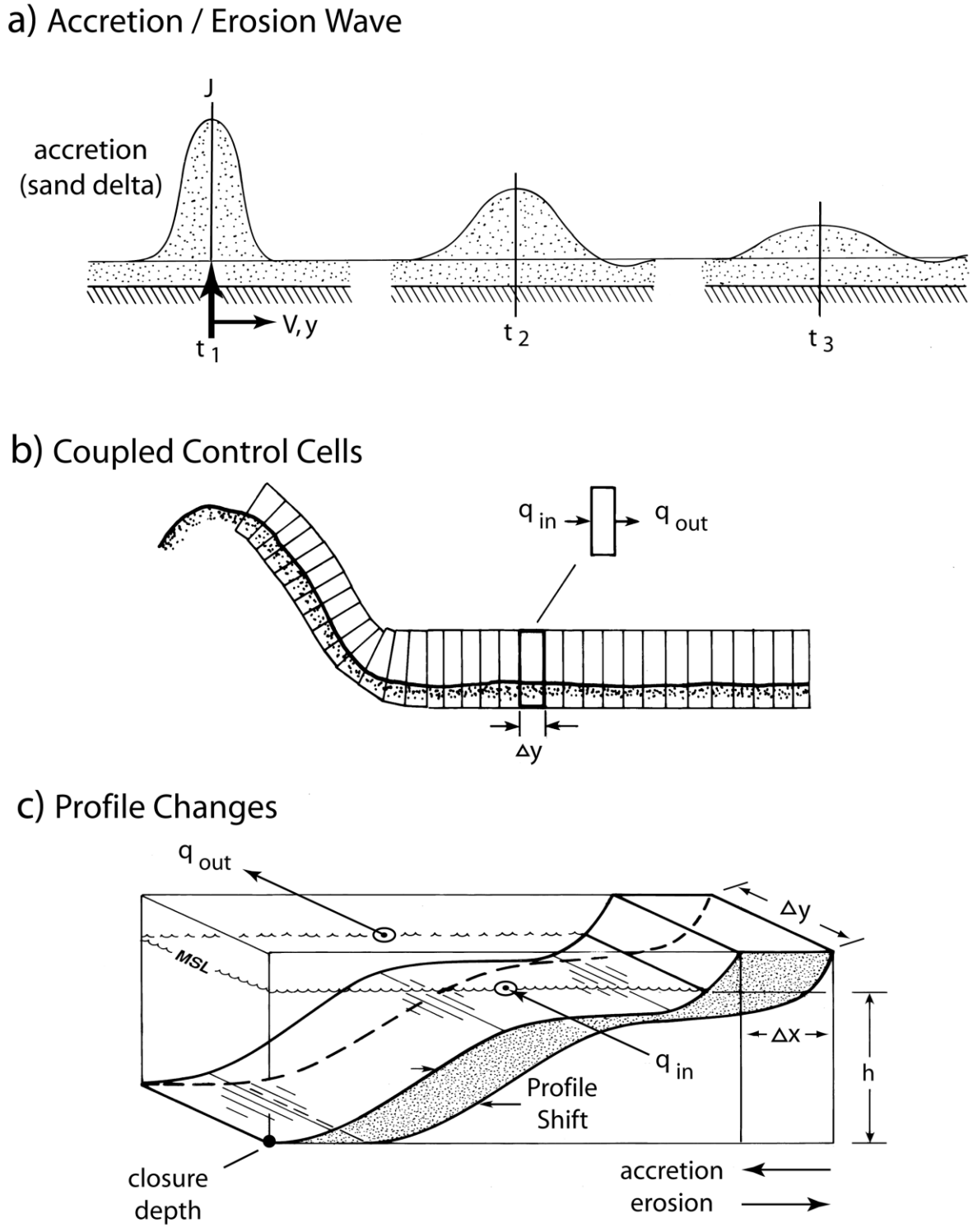

Figure A2: Computational approach for modeling shoreline change after Jenkins, et. al., (2007).

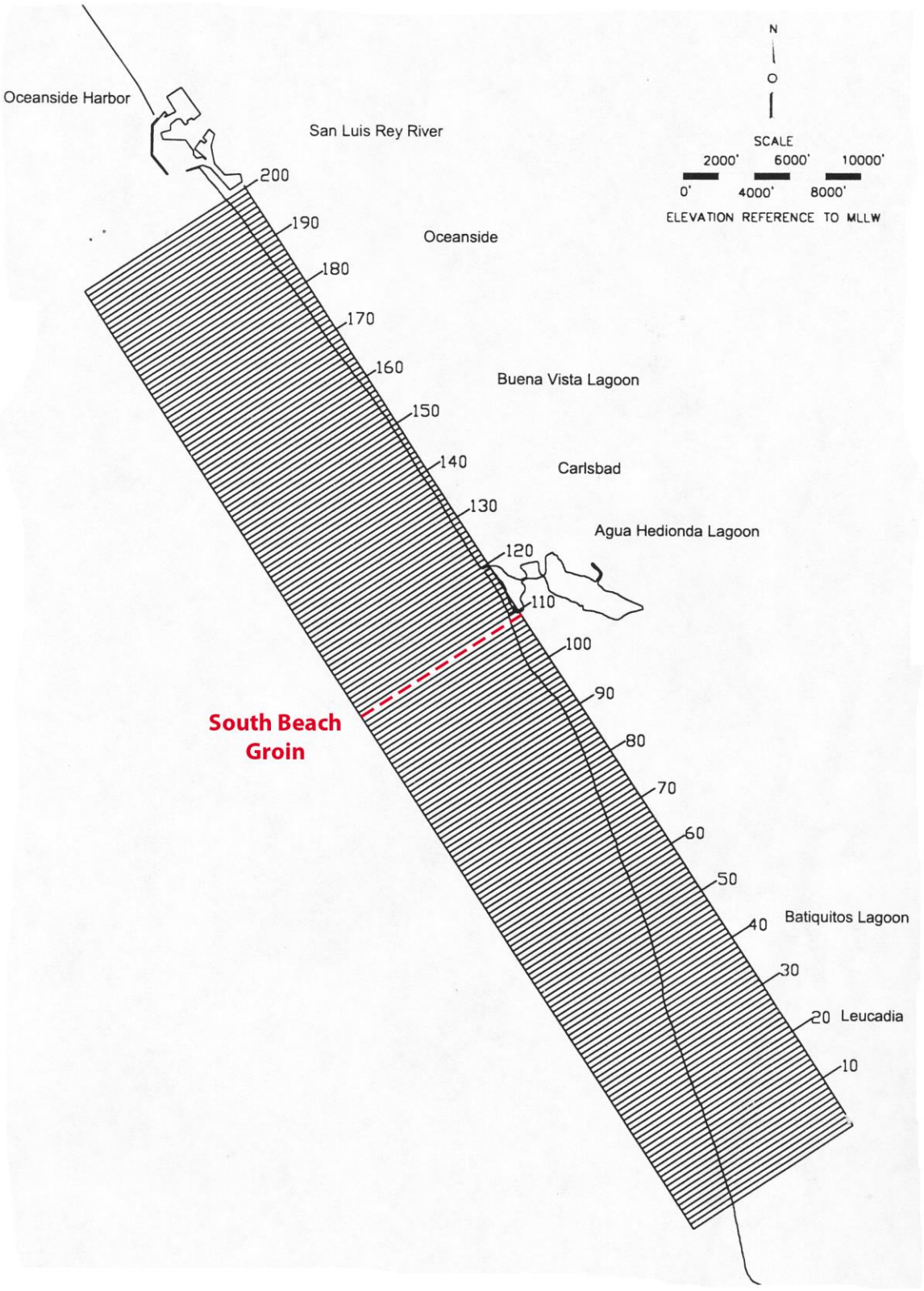

Figure A3: Arrangement of coupled control cells used to model the impacts of removal of the South Beach Groin.

$$\frac{dV}{dt} = J(t) + q_{L1} + q_{RE} - q_{L2} \qquad (2)$$

Sediment is supplied to the control cell by the sediment yield from the rivers, $J(t)$, by the influx littoral drift from up-coast sources, q_{L1} and by new sediment that recharges the system q_{RE} as a consequence of bluff erosion within the control cell. Sediment is lost from the control cell due to the action of wave erosion and expelled from the control cell by exiting littoral drift, q_{L2}. Here fluxes into the control cell ($J(t)$ and q_{L1}) are positive and fluxes out of the control cell (q_{RE} and q_{L2}) are negative. The beach sand volume change, dV/dt, is related to the change in shoreline position, dX/dt, according to:

$$\frac{dV}{dt} = \frac{dX}{dt} \cdot Z \cdot l \qquad (3)$$

where $$Z = Z_1 + h_c \qquad (4)$$

Here, Z is the height of the shoreline flux surface equal to the sum of the closure depth below mean sea level, h_c, and the height of the berm crest, Z_1, above mean sea level; and l is the length of the shoreline flux surface. Hence, beaches and the local shoreline position remain stable if a mass balance is maintained such that the flux terms on the right-hand side of equation (2) sum to zero; otherwise the shoreline will move during any time step increment as:

$$\Delta x(t) = \frac{1}{\Delta y(Z_1 + h_c)} \int \left(\frac{\partial}{\partial y} \left(\varepsilon \frac{\partial q}{\partial y} \right) - V \frac{\partial q}{\partial y} + J(t) \right) dt \qquad (5)$$

where ε is the mass diffusivity, V is the longshore drift , J is the flux of sediment from river sources, Δy is the alongshore length of the control cell, and Z_1 is the maximum run-up elevation from Hunt's Formula. River sediment yield, J, is calculated from streamflow, Q, based on the power law formulation of that river's sediment rating curve after Inman and Jenkins, (1999), or

$$J = \gamma \, Q^{\omega} \qquad (6)$$

where γ, ω are empirically derived power law coefficients of the sediment rating curve from best fit (regression) analysis (Inman and Jenkins,1999). When river floods produce large episodic increases in J, a river delta is initially formed. Over time the delta will widen and reduce in amplitude under the influence of surf diffusion and advect down-coast with the longshore drift, forming an accretion erosion wave (Figure A2). The local sediment volume varies in response to the net change of the volume fluxes, q, between any given control cell and its neighbors, referred to as divergence of drift = $q_{in} - q_{out}$, see Figure A2b and A2c. The mass balance of the control cell responds to a non-zero divergence of drift with a compensating shift, Δx , in the position of the equilibrium profile (Jenkins and Inman, 2006). This is equivalent to a net change in the beach entropy of the equilibrium state . The divergence of drift is given by the continuity equation of volume flux, requiring that dq/dt is the net of advective and diffusive fluxes of sediment plus the

influx of new sediment, *J*. The rate of change of volume flux through the control cell causes the equilibrium profile to shift in time according to (5).

The BCM (Figure A1, lower) models the erosion of country rock by wave action when the sediment cover has been completely eroded away (Jenkins and Wasyl, 2005). Because bedrock cutting requires the near absence of a sediment cover, the boundary conditions for cutting are determined by the coupled mobile sediment model, LCM. When LCM indicates that the sediment cover is absent in a given area, then BCM kicks in and begins cutting. BCM cutting is powered by the wave climate input to LCM but applied only to areas where mobile sediment is absent. Bedrock cutting involves the action of wave energy flux *ECn* to perform the work required to abrade and notch the country rock. Both abrasion and notching mechanisms are computed by the newly developed wave-cutting algorithms. These algorithms use a general solution for the recession *R* (in meters) of the shelf and sea cliff. The recession rate dR/dt is a function of the incident wave energy flux,

$$\frac{dR}{dt} = \frac{\rho}{\rho_s} f_e \, ECn \qquad (7)$$

where ρ is the density of seawater; ρ_s is the density of the bedrock, and f_e is a function that varies from 0 to 1 and is referred to as the erodibility. The units of the erodibility are the reciprocal of the wave force per unit crest length (m/N). The erodibility is given separate functional dependence on wave height for the platform abrasion and wave notching of the sea cliff. For abrasion, the erodibility varies with the local shoaling wave height $H_{(x)}$ as

$$f_e = K_a \Theta_{ij} \, H_{(x)}^{1.63} \quad (\text{abrasion}) \qquad (8)$$

where Θ_{ij} is the bedrock failure shape function and K_a is an empirical constant. Consequently, recession by abrasion is a maximum at the wave breakpoint (at a depth of about 5/4 the breaking wave height, H_b) and decreases in both the seaward and shoreward directions. In contrast, the erodibility of the notching mechanism is a force-yield relation associated with the shock pressure of the bore striking the sea cliff (Bagnold, 1939; Trenhaile, 2002). The shock pressure is proportional to the runup velocity squared, which is limited by wave runup elevation. Wave pressure solutions (Havelock, 1940) give

$$f_e = K_n \Theta_{ij} \, \eta_r^2 \quad (\text{notching}) \qquad (9)$$

where K_n is an empirical constant and the runup elevation 0_r is dependent on the tidal level 0_o and the breaking wave height by Hunt's formula,

$$\eta_r = \eta_o + \Gamma H_b \qquad (10)$$

Here Γ is an empirical constant from Hunt's formula (*Hunt*, 1959).

To quantify the effect of removal of the South Beach Groin on littoral drift and beach stability, we invoke the LCM algorithms of the Coastal Evolution Model (Figure A1) after

initializing for historic wave climate and river sediment flux as detailed in Section 3.. The LCM computational sequence begins with forward refraction calculation using OCEANRDS to solve for the wave height and x and y components of the wave number at each point in the sequence of coupled control cells (Figure A2b and Figure A3). The x and y components of wave number are orthogonalized to compute the significant wave angle in each grid cell relative to the shoreline normal of these near-field computational cells. The calculation is carried shoreward until the wave height meets or exceeds 5/4 the local depth. This condition defines the point of wave breaking. The wave height, H_b wave angle α_b and grid cell location (x_b, y_b) at which this wave breaking condition is met are written into a *breaker file* for use in subsequent potential longshore transport calculations.

The breaker files generated by refraction/diffraction calculations are used to compute the potential longshore transport rates at 6 hour intervals. The formulation for the longshore transport rate is taken from the work of Komar and Inman (1970) according to:

$$q_{L2} = K\left(C_n S_{yx}\right)_b \qquad (11)$$

where q_{L2} is the local potential longshore transport rate; C_n is the phase velocity of the waves; $S_{yx} = E\sin\alpha_b \cos\alpha_b$ is the radiation stress component; α_b is the breaker angle relative to the shoreline normal; $E = 1/8\rho g H_b^2$ is the wave energy density; ρ is the density of water; g is the acceleration of gravity; H_b is the breaking wave height; and, K is the transport efficiency equal to:

$$K = 2.2\sqrt{c_{rb}} \qquad (12)$$

$$c_{rb} = \frac{2g\tan^2\beta}{H_b\sigma^2} \qquad (13)$$

Here c_{rb} is the reflection coefficient which is calculated from a gross estimate of the nearshore bottom slope, as determined from the bathymetry file using the break point coordinates and the position of the 0 MSL contour; and, σ is the radian frequency = $2\pi/T$, where T is the wave period. These equations relate longshore transport rate to the longshore flux of energy at the break point which is proportional to the square of the near breaking wave height and breaker angle. By this formulation, the computer code calculates a local longshore transport rate for each break point locations along the shoreline of the forward refraction grid shown in Figures A3. The potential longshore sand transport rates calculated for these points are ensemble averaged for each 6 hour time step interval within the 1980-2000 simulation period to obtain estimates of the fluxes, q_{L2} in-and-out of the near-field computational cell due to local longshore transport (littoral drift).

We use state-of-the-art, eliptic cycloid algorithms (Figure A4) for the equilibrium beach profile (Jenkins and Inman,2006) to calculate the long term variability of beach profiles along North Beach, Middle Beach and South Beach. The elliptic cycloid was proven to be the mathematical representation of a shore-rise or bar-berm beach profile by Jenkins and Inman, 2006. This mathematical relation is embedded in the algorithms of the Coastal Evolution Model

(Jenkins and Wasyl 2005) and used to calculate the bottom profile of the beach and seabed offshore of North Middle and South Beaches for any given point in time based on the incident wave height, period, direction and sediment grain size. The elliptic cycloid solution is a curve produced by a rolling ellipse (Figure IIa), and allows all the significant features of the equilibrium profile to be characterized by the eccentricity and the size of one of the two ellipse axes. These two basic ellipse parameters are related herein to both process-based algorithms and to empirically based parameters for which an extensive literature already exists. The elliptic cycloid solutions reproduce realistic and validated wave height, period and grain size dependence and demonstrated generally good predictive skill in point-by-point comparisons with measured profiles (Jenkins and Inman, 2006). This analysis takes into account the effects of the wave climate and bi-annual beach disposal of dredged Agua Hedionda sands. The beach profile algorithms are calibrated using pre- and post dredging beach profile surveys from Jenkins and Wasyl (2010) and Elwany, et al, 1999. The calibrated algorithms are then forced by 24 years of continuous wave data using time varying divergence of drift from equation (1) to compute changes in the mean shoreline position from equation (5).

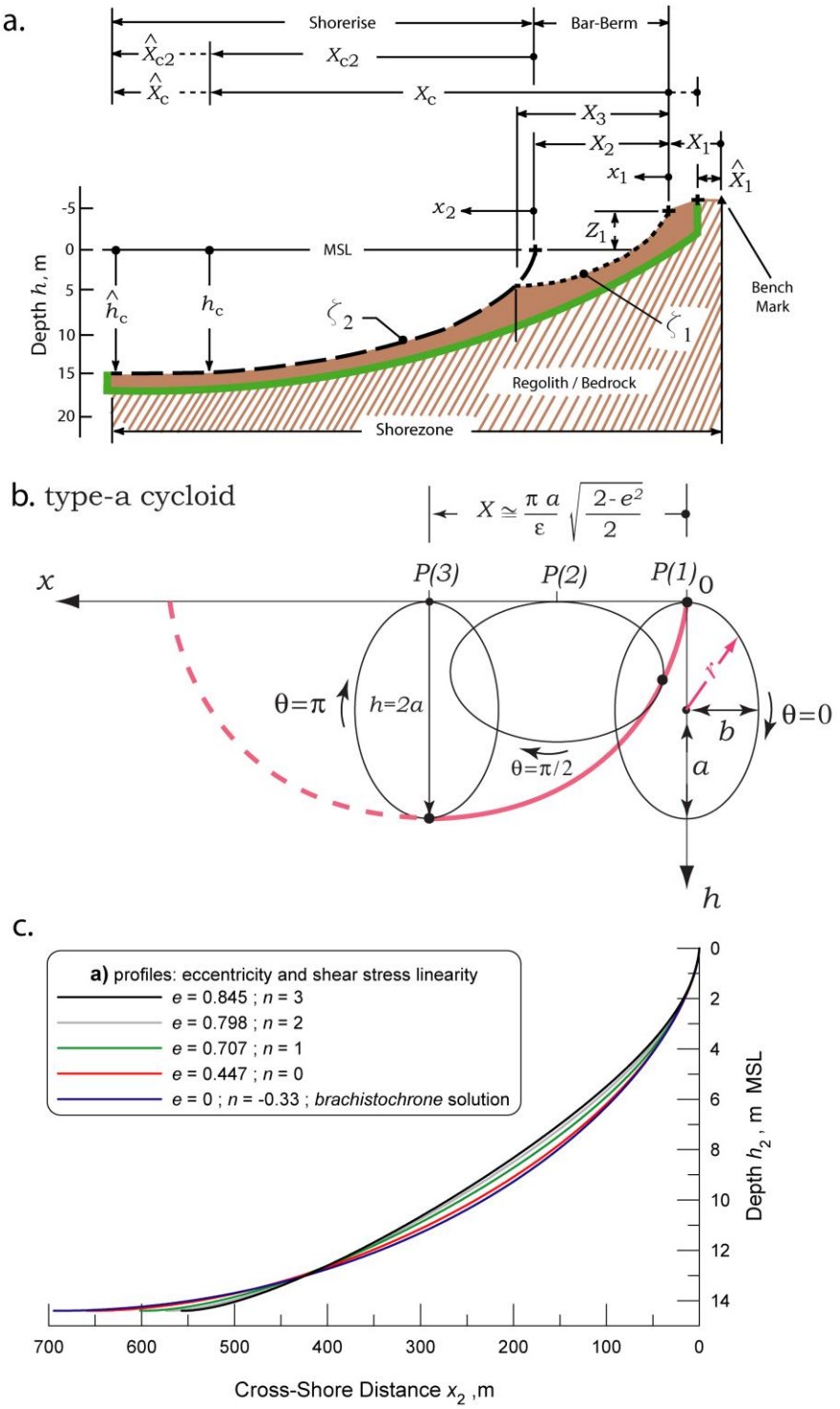

Figure A4. Equilibrium beach profile a) nomenclature, b) elliptic cycloid, c) Type-a cycloid solution.

APPENDIX III. Dredging and Disposal History at Agua Hedionda Lagoon (from Jenkins and Wasyl, 2001)

Dredging And Disposal History							
Year	**Dredging**				**Disposal**	**Comments**	
	Date		**Volume (yds^3)**	**Basin Dredged**	**Volume (yds^3)**	**Location Placed 1**	
	Start	Finish					
1954	Feb-54	Oct-54	4,279,319	Outer, Middle, & Inner	4,279,319	N, M, S	Initial construction dredging
1955	Aug-55	Sep-55	90,000	Outer	90,000	S	Maintenance
1957	Sep-57	Dec-57	183,000	Outer	183,000	S	Maintenance
1959-60	Oct-59	Mar-60	370,000	Outer	370,000	S	Maintenance
1961	Jan-61	Apr-61	227,000	Outer	227,000	S	Maintenance
1962-63	Sep-62	Mar-63	307,000	Outer	307,000	S	Maintenance
1964-65	Sep-64	Feb-65	222,000	Outer	222,000	S	Maintenance
1966-67	Nov-66	Apr-67	159,108	Outer	159,108	S	Maintenance
1968-69	Jan-68	Mar-69	96,740	Outer	96,740	S	Maintenance
1972	Jan-72	Feb-72	259,000	Outer	259,000	S	Maintenance
1974	Oct-74	Dec-74	341,110	Outer	341,110	M	Maintenance
1976	Oct-76	Dec-76	360,981	Outer	360,981	M	Maintenance
1979	Feb-79	Apr-79	397,555	Outer	397,555	M	Maintenance
1981	Feb-81	Apr-81	292,380	Outer	292,380	M	Maintenance
1983	Feb-83	Mar-83	278,506	Outer	278,506	M	Maintenance
1985	Oct-85	Dec-85	403,793	Outer	403,793	M	Maintenance
1988	Feb-88	Apr-88	333,930	Outer	103,000	N	Maintenance
					137,860	M	Maintenance
					93,070	S	Maintenance
1990-91	Dec-90	Apr-91	458,793	Outer	24,749	N	Maintenance
					262,852	M	Maintenance
					171,192	S	Maintenance
1992	Feb-92	Apr-92	125,976	Outer	125,976	M	Maintenance
1993	Feb-93	Apr-93	115,395	Outer	115,395	M	Maintenance
1993-94	Dec-93	Apr-94	158,996	Outer	74,825	N	Maintenance
					37,761	M	Maintenance
					46,410	S	
1995-96	Sep-95	Apr-96	443,130	Outer	106,416	N	Maintenance
					294,312	M	
					42,402	S	
1997	Sep-97	Nov-97	197,342	Outer	197,342	M	Maintenance

APPENDIX III. Continued

Dredging And Disposal History							
Year	**Dredging**				**Disposal**	**Comments**	
	Date		**Volume(yds^3)**	**Basin Dredged**	**Volume (yds^3)**	**Location Placed 1**	
	Start	Finish					
1998	Dec-97	Feb-98	60,962	Middle	60,962	M	Modification dredging
	Feb-98	Feb-99	498,736	Inner	370,297	M	Modification dredging
					128,439	S	
1999	Feb-99	May-99	202,530	Outer	202,530	N	Maintenance
2000-01	Nov-00	Apr-01	429,084	Outer	142,000	N	Maintenance
					202,084	M	
					85,000	S	
2002-03	Dec-02	Apr-03	336,357	Outer	100,907	N	Maintenance
					141,270	M	
					94,180	S	
2004-05	Jan-05	Mar-05	348,151	Outer	104,446	N	Maintenance
					146,223	M	
					97,482	S	
2006-07	Jan-07	Apr-07	333,373	Outer	100,012	N	
					140,017	M	
					93,344	M	Maintenance
Total (Construction + Maintenance)			**12,310,247**		**12,310,247**		
Sub-Total (Maintenance Only)			**7,471,380**		**7,471,380**		

N = North Beach

M = Middle Beach

S = South Beach